ACS OMEGA

Open Access

http://pubs.acs.org/journal/acsodf

Article

Novel Approach of Nanophotonic Electron Transfer for Augmenting Photosynthesis in *Arachis hypogaea*: A Biophysical Rationale behind the Plasmonic Enhancement of Chemical Energy Transfer

Shikha Dhiman, Nitai Debnath, Kaustav Bandyopadhyay, and Sumistha Das*

Cite This: *ACS Omega* 2024, 9, 35332−35347

Read Online

ACCESS | Metrics & More | Article Recommendations | Supporting Information

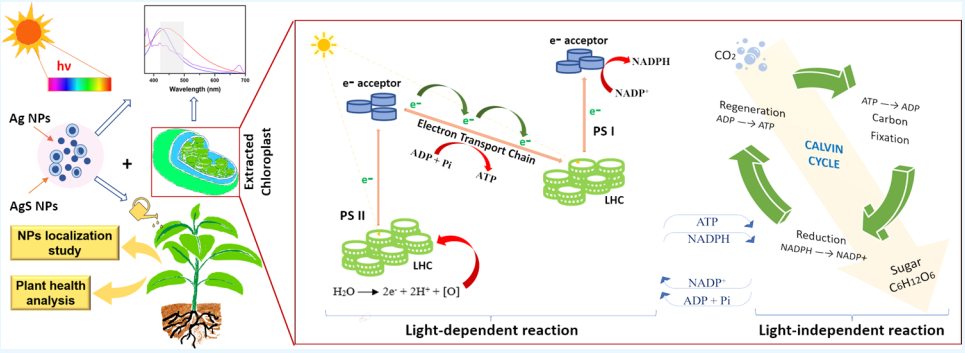

ABSTRACT: Plant photosynthetic machinery is the main source of acquisition and conversion of solar energy to chemical energy with the capacity for autonomous self-repair. However, the major limitation of the chloroplast photosystem is that it can absorb light only within the visible range of the spectrum, which is roughly 50% of the incident solar radiation. Moreover, the photosynthetic apparatus is saturated by less than 10% of available sunlight. If the capacity of solar light absorption and the transmission of resulting photons through the photosynthetic electron transport chain (ETC) can be extended, the overall efficiency of photosynthesis can be improved. The plant nanobionic approach can address this via the introduction of nanoparticles into or in the vicinity of the photosynthetic machinery/chloroplast. We have studied this exceptional nanobionic-mediated capability of two optically active nanostructures and evaluated the impact of their optical properties on plant photosynthesis. Our study revealed that metal (Ag) and core−shell metal nanostructures (AgS) can increase light absorption and improve electron transport through ETC. Both nanostructures were found to have a beneficial effect on the photoluminescence property of the isolated chloroplast. Translocation studies confirmed systemic transportation of the nanomaterial in different plant tissues. The primary growth parameters showed no detrimental effect until 21 days of treatment on *Arachis hypogaea*. The nano silver/silica core/shell structure (AgS) was found to be more advantageous over nano silver (AgNP) in photon entrapment, light-dependent biochemical reactions, and toxicity parameters. In the future, these nanostructures can enhance photosynthesis by increasing light absorption and resulting in higher assimilatory power generation in the form of ATP and NADPH. This approach may lead to a paradigm shift toward a sustainable method for the configuration of plant chloroplast-based hybrid energy harvesting devices.

INTRODUCTION

In the biological realm, plants have developed the most fundamental and essential physiological mechanism for energy entrapment, known as photosynthesis.[1] The unique ultrastructural merit of plant cells and organelles has made them scientifically attractive in the last few years to develop bio-interfacing devices using nanostructures; this technology is precisely known as plant nanobionics. Chloroplasts are the organelles where chemical energy is produced in green plants. The captured solar energy is then employed as the fundamental unit to regulate various physiological processes by plants and is taken forward to the ecosystem in the form of chemical energy. For photosynthesis to occur, two sets of processes—light-dependent reactions and light-independent CO_2 fixation—take place to produce glucose as the final product.[2] The range of wavelengths at which chloroplasts can absorb solar irradiation is rather narrow. Less than 10% of the sunlight is used by plants' photosynthetic assembly[3] and therefore leaves room for improvement in the solar energy conversion efficiency for augmented photosynthesis and

Received: January 17, 2024
Revised: July 2, 2024
Accepted: July 8, 2024
Published: August 8, 2024

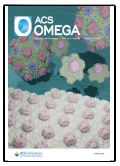

utilization of acquired energy further. Expanding the spectrum of solar light absorption is of utmost importance to increase photosynthetic efficiency.[4]

A huge number of studies have already shown that many of the engineered nanoparticles (NPs) have distinct optical, electronic, and absorption spectra that expand into the ultraviolet, visible, and near-infrared ranges.[5] Nanomaterials, due to their unique characteristics and increased stability, can create chloroplast−nanomaterial-based photocatalytic stable assemblies with enhanced features for both in vivo and ex vivo conditions.[6] It is also evident that neither the chloroplast absorbs the full amount of solar radiation in nonsaturating light situations nor all of the absorbed photons are engaged in electron transfer under intense light conditions.[7,8] NPs can interfere with and modulate capacity for photosynthetic energy production, photochemical fluorescence, and quantum yield depending on chloroplast-mediated light-harvesting capacity.[9] In keeping with the value of the process, scientists tried either to artificially duplicate the natural process of photosynthesis or to increase its efficiency in plants utilizing interference of nanotechnology.

There are several studies on the improvement of photosynthetic activity in plants. For example, by introducing carbon nanotubes (CNTs) into the chloroplast, plants have been reported to enhance capturing light energy.[7] Scientists have also experimentally proved that the chloroplast is able to collect light wavelengths beyond the limited range, such as in ultraviolet, green, and near-infrared, in the presence of CNTs, which act as artificial antenna elements.[6,10]

In addition to the theory of nanomaterial-induced photon absorption, Govorov et al. came up with a very interesting finding that revealed that metal NPs have additional potential to modulate solar light absorption and thereby convert light energy into chemical energy in a nanomaterial-based hybrid artificial photosynthetic model system.[11] Surface plasmon resonance (SPR) is a well-known attribute of metal NPs in a size-dependent manner. In the presence of metal NPs (Ag and Au), incident photons of appropriate wavelength induce generation of resonating surface polaritons. These excited polaritons were combined with light-absorbing chlorophyll molecules, resulting in an improved photocurrent response. The dual effect of SPR and electron−hole separation have been shown to boost the generation of excited electrons[11] in the artificial light-harvesting photosynthetic model system. According to Govorov et al., this new hybrid system has the potential to produce 10 times as many excited electrons.[11]

Core/shell nanostructures (CSNs) have captured scientific attention in various fields including imaging, photonics, and advanced agriculture due to their unusual features resulting from their shape, core geometry, shell structure, and different blends of core and shell arrangements.[12] CSNs not only compensate for some of the shortcomings of bare NPs but also amplify several other properties. The goals of coating the core NPs are several, including surface modification, the potential to increase stability, efficiency, porosity, and dispersibility, controlled core release, reduced consumption of rare elements, etc.[13] For example, Negishi et al. reported that incorporating TiO_2 into Au/Pb CSNs significantly increased water oxidation activity.[14] When compared to uncoated CeO_2 NPs, polyvinylpyrrolidone (PVP)-coated CeO_2 NPs improved stomatal conductance. Also, increased stomatal conductance indicated that CeO_2 NPs had a positive role in gas exchange in soybeans.[15] For photocatalytic water splitting, Zhang et al. used platinum-modified graphitic carbon nitride,[16] whereas Zheng et al. used hollow CSNs to separate oxidation and reduction centers for the same effect.[17] In another example, Li et al. developed reduction-cocatalyst Pt NPs onto the inner shell surface of hollow carbon nitride spheres, while oxidation-cocatalyst Co_3O_4 NPs were on the outer shell surface. This conjugate considerably improved photocatalytic activity for H_2 and O_2 evolution.[18] In a similar study,[19] the nanosized silica compound attached to PSII initiated the constant activity of the photosynthetic oxygen-evolving process, demonstrating light-driven electron transport from water to quinone molecules.

In natural photosynthetic machinery (isolated plant chloroplast) using single-walled carbon nanotubes (SWNTs), Giraldo et al. showed for the first time that specific localization of these optically active nanomaterials could have a beneficial impact on photosynthetic activity and electron transport rate.[6] In other nanobionic studies, researchers have also shown that this property of SWNTs can be utilized for their localization in the chloroplast, leading to the development of photonic chemical nanosensors.

Our previous communication revealed that Au nanocrystals localized around chloroplast molecules can promote light absorption and enhance photosynthetic electron transport and ATP synthesis, resulting in improved overall plant development.[20] Bare noble metal nanocrystals (Au and AgNP) can increase the photosynthesis rate. Core/shell nanostructures of these noble metals have the potential to further increase photosynthetic efficiency.[11] Also, theoretically, it has also been shown that SPR peaks of silica/Ag and silica/Au CSNs shifted to 670 and 680 nm, respectively, and coincided with the absorption maxima (673 nm) for the chloroplast photosystem reaction center. As a result, CSNs of Ag and Au were much more suited for augmenting photosynthesis.[12] Zhang et al. investigated the effect of Ag/SiO_2 CSNs on the expression of the secondary plant metabolite artemisinin from a hairy root. This study also exhibited that CSNs had the potential to improve plant growth and production.[16]

All these findings are the impetus behind our study to investigate the role of optically active silver NPs (AgNPs) and core/shell silver/silica NPs (AgS) in light harvesting and the photosynthetic light and dark reaction in a plant chloroplast model system along with their effect on the growth parameter in a plant model system. Many NPs have been engineered to have low or negligible toxicity, which is probably the most desirable property when considering application of NPs for agriculture. Here, we showed that due to the shift in plasmon resonance, the chemical energy production rate and generation of electrons inside the photosynthetic complex can be significantly enhanced by coating. Smaller size distributions and enhanced photostability of the core/shell silver/silica nanostructure made them a better alternative than bare AgNPs for such applications. The studies reveal the possibility of using core/shell AgS as a robust novel material in the expanding field of plant photobiology.

EXPERIMENTAL SECTION

Synthesis of Nanoparticles. AgNPs were synthesized by a simple wet reduction method reported by Radziuk et al. with some modifications.[21] 1 mL of trisodium citrate (30 mM) was mixed with silver nitrate (0.25 mM, 100 mL) and sodium borohydride (10 mM, 3 mL). This solution was heated at 80 °C and kept undisturbed for 2 h after heating. The color of the

https://doi.org/10.1021/acsomega.4c00550
ACS Omega 2024, 9, 35332−35347

solution changed to light brownish yellow, confirming the synthesis of silver colloid. The as-prepared silver colloid was further cooled and centrifuged at 5000 rpm for 20 min. The pellet was washed with deionized water (DW). The dispersed NPs were stored at 4 °C for further investigation.

For AgS synthesis,[22] 8 mL of as-prepared AgNPs were dispersed in 20 mL of deionized water. 200 mL of propane-2-ol and 3.2 mL of ammonium hydroxide were added further to the dispersion. It was followed by dropwise addition of 200 μL of tetraethyl orthosilicate (TEOS), and stirring was continued for 30 min. The solution was then kept undisturbed at 4 °C for overnight. The next day, centrifugation at 3000 rpm was carried out, followed by repeated washing with a 5:4 water−ethanol mixture. Finally, AgS was air-dried for future use.

Physicochemical Characterization of Nanoparticles. Synthesized AgNPs and AgS were characterized using microscopic and spectrophotometric techniques. The detailed methodology for sample preparation is available in the Supporting Information (SI) section.

Stability Study. The stability of these synthesized nanostructures was thoroughly studied using thermal gravimetric analysis (TGA), ζ potential, and hydrodynamic radius analysis in different experimental situations. The detail of the method utilized is elaborated in the SI section.

Photosynthesis Study. *Isolation of the Chloroplast.* The chloroplast was isolated from leaves following Gerwick.[23] For this, fully inflated *Arachis hypogaea* leaves were divided into smaller pieces and blended for 15 s in a solution containing 330 mM mannitol, 30 mM HEPES, 2 mM EDTA, 3 mM $MgCl_2$, and 0.1% w/v BSA (pH 7.8). After filtration of the slurry through three layers of cheesecloth, it was centrifuged for 5 min at 250*g*. The supernatant was further centrifuged at 1000*g* for an additional 5 min.[23] The chloroplast pellet was cleaned and resuspended in an extraction buffer before being used to study the photosynthetic pathway.

Light-Dependent Reaction. *Measurement of the Hill Reaction.* Water splitting by light in the absence of CO_2 is known as the Hill reaction. Hill activity was assayed according to the method of Vishniac.[24] For this, 1 mL of chloroplast solution was mixed with 4 mL of sucrose−phosphate buffer. Then, 0.5 mL of 0.03% 2,6-dichlorophenolindophenol (DCPIP) was added to a 6-well transparent plate. Absorbance was recorded at 620 nm after light irradiance for 2 min. This treatment was carried out in a lightbox equipped with photosynthesis-specific cool fluorescent bulbs. Reactions in the dark resulted in pigment depletion due to another nonphotosynthetic event, which was subtracted from the total absorbance to obtain the net light depletion for treatment only. The net reduction due to the Hill reaction was expressed as μMole DCPIP decreased/min. The same method was repeated with different concentrations (10, 100, 1000, 10, and 100 ppm) of AgNP and AgS solutions. The whole set of experiments were repeated at least three times.

Photophosphorylation. The change in ferricyanide and NADP was determined spectroscopically by the Trebst method.[25] Ferricyanide reduction was measured using a mixture containing the chloroplast (10 μg chloroplast/mL), 86 mM sorbitol, 50 mM tricine (pH 8.1), 50 mM NaCl, 5 mM $MgCl_2$, 2 mM K_2HPO_4, 2 mM ADP, and 1 mM ferricyanide. Immediately after 1 min of saturated irradiation, trichloroacetic acid (TCA) was added to a final concentration of 1.8%. Chloroplasts were pelleted by centrifugation, and the absorbance of the supernatant was measured at 420 nm.[25] The dark control did not show any reduction of ferricyanide.

The experimental conditions for measuring the NADP reduction were the same, except for the removal of ferricyanide from the reaction mixture and the addition of 3 μM purified spinach ferredoxin (from Sigma) and 0.66 mM NADP. After irradiating for 1 min, the reaction mixture was centrifuged, and a change in absorbance was recorded at 340 nm.

ATP Synthesis Analysis. Light-induced ATP production in chloroplasts was quantified by comparing the level of ATP in the dark and 1 min after illumination. For this, 1 mL of the reaction mixture containing 0.4 M sucrose, 50 mM Tris-HCl (pH 7.6), 10 mM NaCl, 5 mM $MgCl_2$, 2 mM ADP, 10 mM Na_2HPO_4, and undamaged chloroplast was taken in a 6-well plate. The dark control and light-illuminated samples were immediately treated with 10% TCA and neutralized with 3 M Na_2CO_3 later.[26] The ATP Colorimetric Assay Kit (Elabscience) was used for the ATP content assay.

Oxygen Evolution. Oxygen evolution was assayed in a medium consisting of 0.33 M sorbitol, 2.0 mM NaEDTA, 1.0 mM $MgCl_2$, 1.0 mM $MnCl_2$, and 50 mM HEPES. 0.88 mM 2,6-dichlorophenolindophenol (DCPIP) served as an oxidant in all assays and was added to the medium immediately prior to administration of the chloroplasts. The reaction was illuminated for 1 min with visible light (400−700 nm).[27] Oxygen evolution was measured in a Clark-type oxygen electrode (Hansatech).

Photoluminescence Spectroscopy. To understand the impact of NPs on photon absorption, the isolated chloroplast was dispersed in different AgNP and AgS samples. The same concentration of NP solution (200 μL) was added to different volumes of the chloroplast solution, and the corresponding photoluminescence (PL) spectra were recorded at room temperature using an Agilent Cary Eclipse spectrofluorometer.

Similarly, PL spectra were obtained with chlorophyll treated with different concentrations of AgNPs and AgS. Here, the amount of chlorophyll was constant. The PL spectra were recorded to understand the effect of NPs on plant photon absorption using a high-resolution spectrofluorometer.

Light-Independent Reaction. *Carbon Assimilation Assay. NADP-glyceraldehyde-3-phosphate Dehydrogenase (GPDHase) Activity.* The method described by Taylor et al. was used to measure the NADP-glyceraldehyde-3-phosphate dehydrogenase (GPDHase) activity in chloroplasts.[28,29] The enzyme was activated by addition of 0.1 mL of the isolated enzyme extract to a reaction mixture containing 0.2 M tricine (pH 8.4) and 20 mM ATP. After incubation for 5 min, another reaction mixture consisting of 62.5 mM tricine (pH 8.4), 16 mM $MgCl_2$, 7.8 mM ATP, and 0.2 mM NADH was added. The oxidation of NADPH was then observed at 340 nm after the addition of 50 mM glycerate 3-P to initiate the reaction.

Fructose-1,6-bisphosphatase (FBPase) Activity. Preincubation of the enzyme extract with the reaction medium containing 0.14 M tricine (pH 7.9), 14 mM $MgCl_2$, 7 mM DTT, and fructose-1,6-bisphosphatase (FBPase) was carried out for 10 min. Post incubation, 60 mM fructose-1,6-bisphosphate was added to the primary solution. After 15 min, 0.5 mL of 10% (w/v) TCA was added to end the reaction. To quantify the enzyme activity, the absorbance was recorded at 340 nm after centrifugation for 10 min at 12,000*g*.

Uptake and Translocation Study of AgNPs. *Microscopic Analysis of NP Translocation. Synthesis of FITC-Tagged NPs.* For investigation of NP uptake in a plant system,

https://doi.org/10.1021/acsomega.4c00550
ACS Omega 2024, 9, 35332−35347

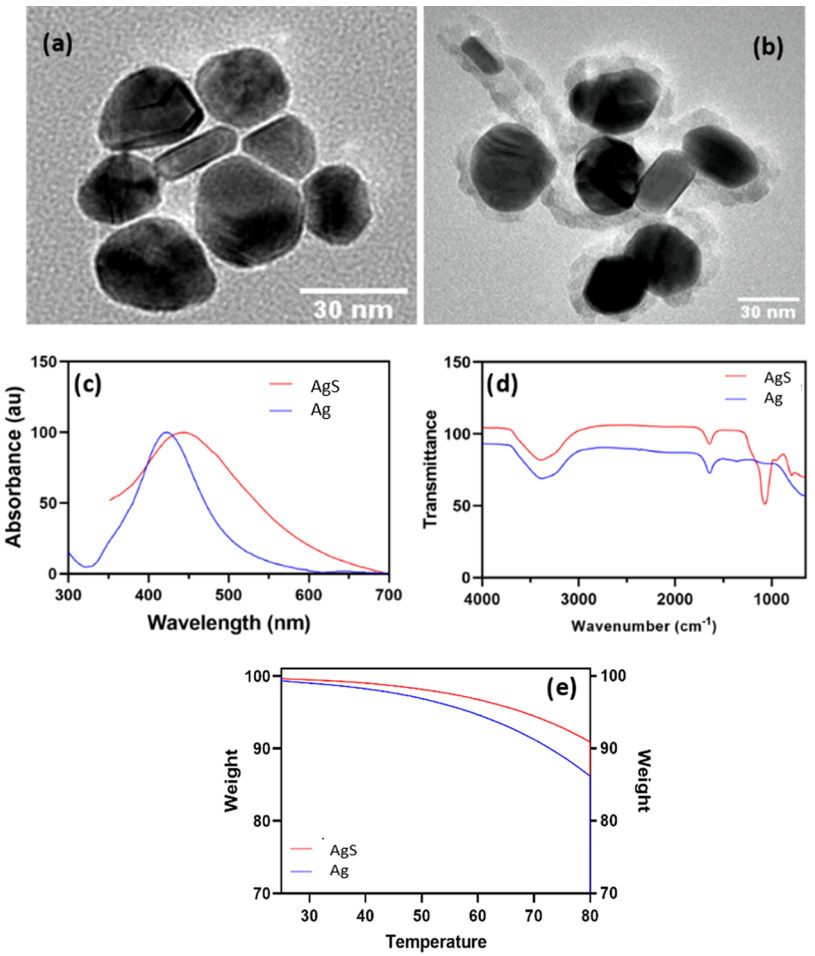

Figure 1. HR-TEM image of (a) AgNPs and (b) AgS (silica coating visible in gray contrast). (c) UV−vis spectra of AgNPs and AgS showing a red shift. (d) FTIR spectra of AgNPs and AgS clearly showing Si−O−Si stretching. (e) TGA analysis of AgNPs and AgS.

fluorescein-B-isothiocyanate (FITC)-tagged AgNPs (AgNP-FITC) were synthesized. To make AgNP-FITC, AgNPs were first amine-functionalized by co-condensation of 3-amino-propyltriethoxysilane (APTES). For this, 0.5 g of AgNPs were dispersed in about 50 mL of DMSO for about 30 min in an ultrasonic bath. After addition of 400 μL of APTES to the dispersion, the mixture was refluxed at 120 °C for about 3 h, followed by centrifugation at 12,000 rpm for 15 min and washing of the pellet several times with ethanol. Finally, the product was dried at 60 °C overnight to obtain amine-functionalized AgNP.

For preparing FITC tagging on amine-functionalized AgNPs, aminated AgNPs were dispersed in 0.1 M Na_2CO_3 buffer. 1 mg of FITC dissolved in 2 mL of DMSO was immediately added to this, and the reaction mixture was stirred at room temperature for 24 h in the dark. FITC-labeled AgNPs (AgNP-FITC) were recovered by centrifugation at 10,000 rpm at 4 °C. Pellets were washed repeatedly and dispersed in distilled water to remove excess FITC.

Translocation Study of Fluorophore-Coated NPs in Plants. AgNP-FITC exhibited much stronger fluorescence than AgNPs alone. Therefore, the AgNP-FITC dispersion was used for the plant uptake study. For this, FITC-tagged AgNPs were dispersed in water and used for the uptake study with incubation of groundnut seedlings for 24 h. For this, 15-day-old seedlings were taken in a conical flask and incubated in fluorescent NP solution with their root under submerged conditions. Finally, the plants were removed and washed thoroughly with water. Thin cross sections of leaf, petiole, and root samples were obtained manually. Finally, the samples were fixed with glycerol, and sectioned samples were observed under a fluorescence microscope under an FITC filter. The same protocol was also employed for the confocal imaging of the sample. A Nikon eclipse Ts2R-FL microscope was used for fluorescence microscopy, and a Nikon eclipse TI2 A1R model was used for confocal microscopy imaging for in vivo FITC-tagged NP studies.

Ag^+ Release Study by ICP-MS. Ag^+ release from the NP-treated plant was monitored using the inductively coupled plasma mass spectroscopy (ICP-MS) technique at pH 7. For in vivo ICP-MS measurement, AgNPs were sprayed on the plant samples at a dosage of 100 ppm. After 15 days of growth, the leaf and root samples of both treated and control plants were collected and dried in an oven at 37 °C. 1 gm of the dried sample was subjected to digestion using the standard procedure and calibrated against the Ag standard. Then, ICP-MS was used to assess the concentration of Ag to understand the uptake and translocation of NPs in plants.

Fluorescence Intensity Measurement. The experiment was designed to study the change in the fluorescence intensity of chloroplasts in vivo. For this, four fully grown leaves together with the petiole from the top were taken and kept in different treatments for 72 h. The leaves were dipped in a microfuge tube containing 2 mL of dispersions each of Ag,

https://doi.org/10.1021/acsomega.4c00550
ACS Omega 2024, 9, 35332−35347

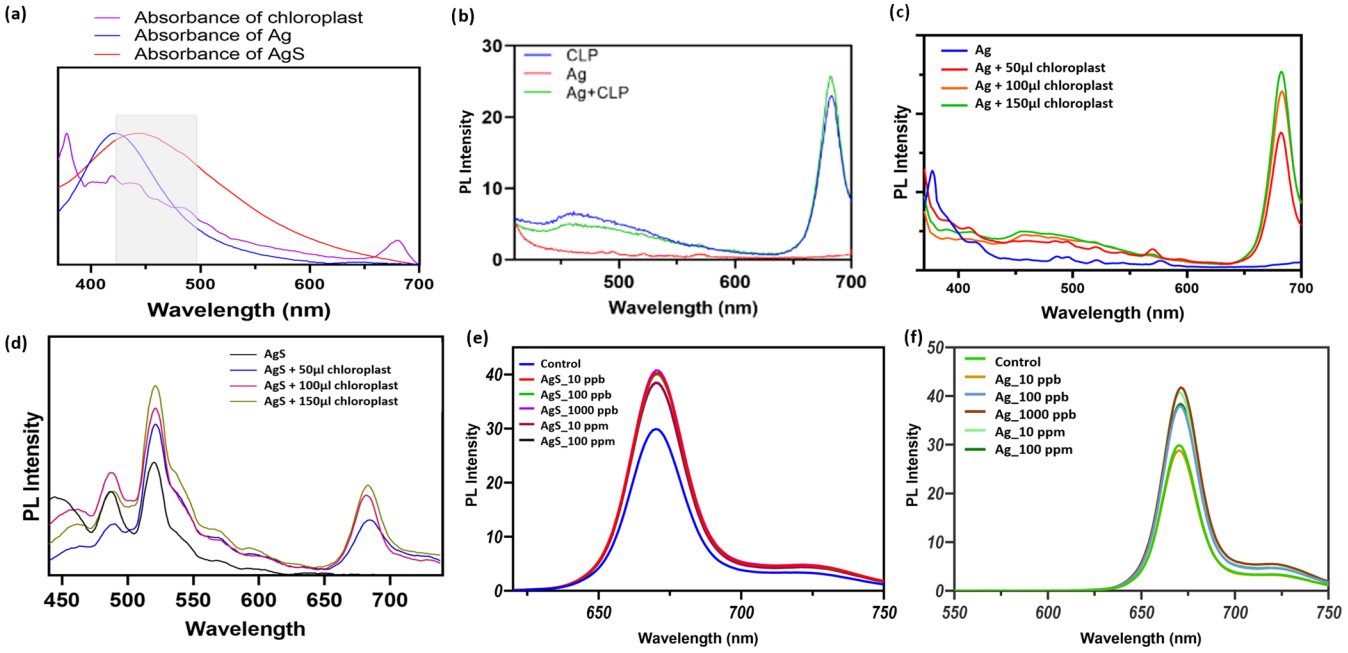

Figure 2. UV−vis absorption spectra. (a) AgNPs and AgS showing a red shift in the SPR of AgNPs after coating with silica. This absorption spectrum overlaps with the absorption maxima of the chloroplast (shown in the shaded column). Photoluminescence emission spectra representing (b) an increase in CLP emission after introduction of AgNPs, (c) AgNP emission with a gradual increase in chloroplast amount, (d) AgS emission with a gradual increase of chloroplast, (e) chlorophyll treated with increasing concentration of AgS, and (f) chlorophyll treated with increasing concentration of AgNPs.

AgS, and AgNP-FITC in Hoagland solutions. The control set was dipped in Hoagland solution only. Leaves were taken out, covered with foil, and kept in the dark for 72 h. After 3 days, the leaves were homogenized in an isolation buffer to extract the chloroplast. After filtration and centrifugation steps, the supernatant was read for fluorescence intensity at 420 nm excitation using a multimode plate reader (TECAN INFINITE M Plex).

Toxicity Study. The toxicity analysis of nanomaterials with application potential in the nanobiointerface is of paramount importance. In our study, not only the entry of NPs within the plant system but also the analysis of plant growth parameters and the development of reaction oxygen species (ROS) in the plant were carried out. The detailed protocol of this section is available in the SI section.

The toxicity of AgNPs and AgS was further investigated in a human breast cancer cell line (MDA-MB-231) using an MTT assay. This methodology is also described in the SI section.

RESULTS AND DISCUSSION

Characterization of Synthesized Nanoparticles. The morphology of both coated and uncoated AgNPs was studied by high-resolution transmission electron microscopy (HR-TEM). The results clearly showed the formation of the SiO_2 shell around the surface of the AgNP. The core and shell diameters of NPs were determined by measuring the difference in contrast of the TEM images. The average particle size of AgNPs and AgS was found to be 30 and 50 nm, respectively (Figure 1a,b).

The SPR peaks of AgNPs and AgS were obtained at 418 and 447 nm, respectively (Figure 1c). In this case, the absorption band of SPR shows a red shift and a broadened peak for AgS, which is an indication of the larger coverage of AgNP core surfaces by silica molecules. The surface functionality of synthesized NPs was confirmed by the FTIR spectrum (Figure 1d). The surface of the AgNP was covered with hydroxyl groups, which was signified by O−H stretching at 3400 cm^{-1}. The C═O stretching was observed at 1640 cm^{-1}. The additional band observed in AgS NPs at around 1073 cm^{-1} is due to Si−O−Si stretching, confirming successful conjugation.

Stability Study (TGA, ZETA, and DLS). The TGA results (Figure 1e) for Ag and AgS revealed that they were highly stable at temperatures ranging from 25 to 80 °C (this range of temperature is beyond the requirement of plants). The samples did not begin to disintegrate or react within the temperature range specified. The weight loss for Ag and AgS was majorly due to water loss during heating.

The tendency for the particles to attract and come together (hence the chance of agglomeration) would be absent if all of the particles in a suspension had a strong negative or positive ζ potential, as the particles would repel each other. The dispersion would resist flocculation, and the colloidal system would be stable if the particle repulsion was strong enough. From the data, it was observed that the ζ potential for AgNPs was found to be −22 mV, and for AgS, it was −21 mV. Both values stated that the NPs are highly dispersed and stable. The slight decrease in the ζ potential of AgS is due to the decrease in the positive charge present on AgNPs before coating.

To ensure that the NP suspensions were stable, the samples were examined using the DLS technique over a time period of 5 days. Data were collected on days 1, 3, and 5 for both NPs dispersed in distilled water. For AgNPs, after 3 days, the average hydrodynamic diameter grew from 166.4 to 171.4 nm and then from 171.4 to 172.6 nm on day 5. The increase in diameter was due to some aggregation of AgNPs, but the difference was not significant, indicating that the sample suspension was quite stable. Similarly, for AgS, the diameter grew from 351.7 to 356.4 nm on the third day and to 366 nm

https://doi.org/10.1021/acsomega.4c00550
ACS Omega 2024, 9, 35332−35347

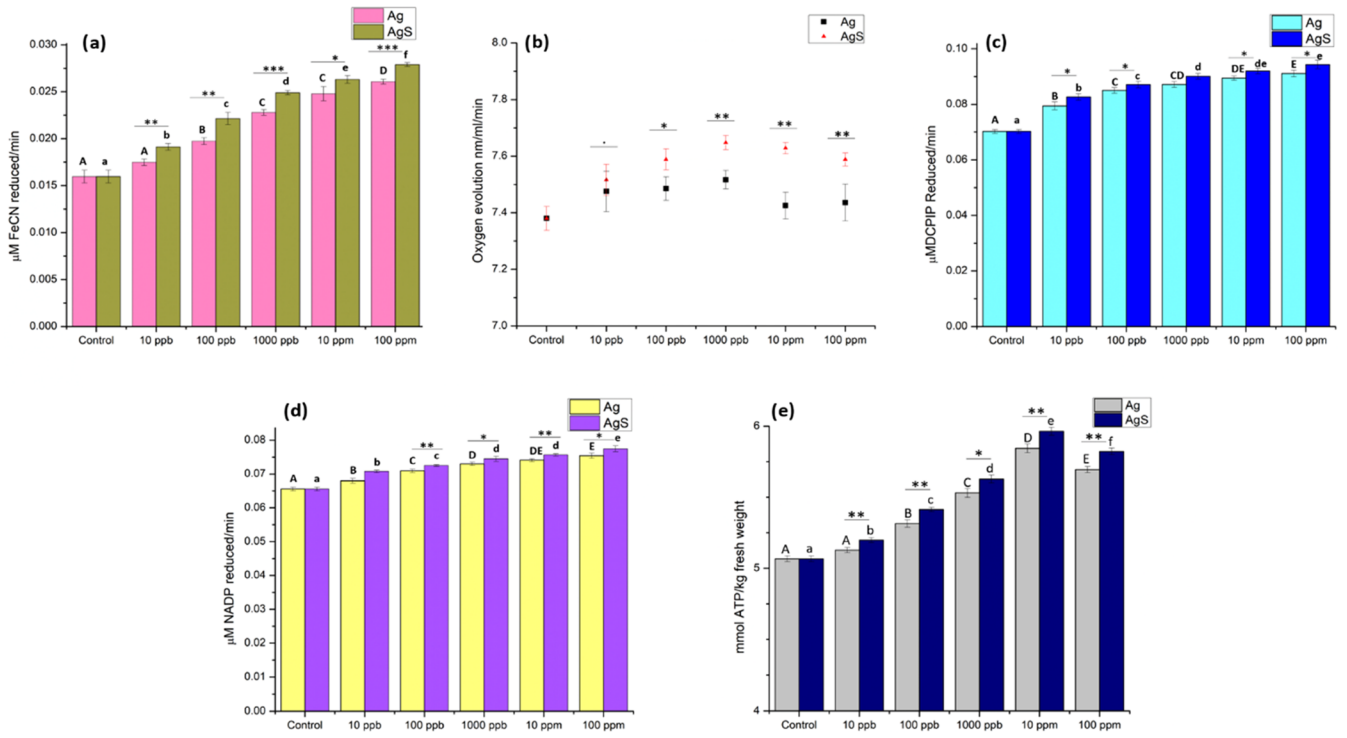

Figure 3. Biochemical changes in the photosynthetic pathway in AgNP- and AgS-treated chloroplasts. (a) Ferricyanide reduction [Ag $F = 102.3$, $P < 0.001$; AgS $F = 256.8$, $P < 0.001$]. (b) Change in oxygen evolution [AgNP $F = 7.274$, $P < 0.01$; AgS $F = 22.4$, $P < 0.001$]. (c) Hill reaction in treated chloroplasts [AgNP $F = 177.2$, $P < 0.001$; AgS $F = 194.9$, $P < 0.001$]. (d) NADP reduction [AgNP $F = 126.9$, $P < 0.001$; AgS $F = 182.3$, $P < 0.001$]. (e) Activity of ATPase [AgNP $F = 449.2$, $P < 0.001$; AgS $F = 713.1$, $P < 0.001$]. Within each type of treatment, mean data (±SE, $n = 3$) followed by the same uppercase letter are not significantly different for a particular dose of AgNPs; within AgS treatment, means followed by the same lowercase letter are not significantly different (Tukey–Kramer HSD test).

on the fifth day (Table S1 in the SI section). The cumulative result indicates the use of the nanostructures to be stable, but sonication is required before bioassays.

Effect of AgNP and AgS on Photosynthesis. *Spectrophotometric Analysis of the NP–CLP Complex.* Acquisition, conversion, and storage of energy are among the basic challenges of civilization over time. If the capacity of solar light absorption by the photosynthetic pigment can be extended, then the photosynthetic efficiency can be improved. The strong enhancement of electromagnetic fields generated through plasmon resonances in metal films and nanoparticulate form has in recent times stimulated considerable interest in photobiology and photosynthesis. The plasmon effect can increase the generation of electrons inside the photosynthetic complex. Here, we have shown a biophysical rationale behind the transfer of excited electrons from SPR active metal nanostructures to chloroplast (CLP) machinery. AgNPs and AgS showed SPR peaks at 418 and 447 nm, respectively (Figure 2a). The red shift in the absorption maxima of AgNPs caused by the formation of the silica shell resulted in a clear overlap in the absorption maxima of chlorophyll and AgS. Hence, AgS showed potential to enhance light absorption more with respect to naked AgNPs.

When a molecule gets excited by irradiation with a specific wavelength, it absorbs energy and emits energy at a different wavelength, which is usually in a longer range due to energy dissipation.[30] The 685 nm fluorescence emission spectra in the chloroplast are a result of antenna chlorophylls linked with the PSII reaction center.[31] Most of this fluorescence is caused by excitation energy transferred from light-harvesting chlorophyll-pigment complexes associated with reaction-center polypeptides.[31] To prove the effect of these NPs in electron exchange, we carried out the PL emission spectral analysis of the CLP nanoconjugate in detail. AgNPs and AgS themselves were found to be luminescent in nature and exhibited blue luminescence under exposure to UV light (Figure S1 in the SI section). PL spectra for AgNPs and AgS were studied at excitation wavelengths of 365 and 380 nm, respectively. It was observed from the graph (Figure 2b) that the chlorophyll emission peak was at 680 nm, and this peak was intensified with addition of AgNPs to CLP solution. The same pattern was also observed with the gradual addition of CLPs to a constant amount of AgNPs (Figure 2c). A similar trend was also reported by Chandra et al.[9] The gradual decrease in emission spectra at 400–450 nm in the case of AgNPs indicated energy transfer from NPs to CLPs. This also indicated the formation of a stable assembly of NPs after being adsorbed on the surface of CLP. In the case of nano AgS (Figure 2d), different spectral patterns having more than one emission peak were obtained due to Ag/silica core/shell structure formation. With addition of 50 μL of CLPs to nano AgS, initially, a slight decrease in the emission spectrum at around 450–500 nm and a simultaneous increase in the 680 nm CLP peak was observed like the AgNP emission spectral pattern illustrated (Figure 2c). This excitation-dependent emission spectra of the CLP–NP conjugate also revealed a different phenomenon with gradual addition of CLP (at or beyond 100 μL). Herein, the emission peak in 525 nm was found to be increased in intensity. This was due to the absolute overlapping absorption spectra of AgS with CLP, resulting in generation of a single peak of the highest intensity (525 nm). To further prove that the increase in CLP emission peak

https://doi.org/10.1021/acsomega.4c00550
ACS Omega 2024, 9, 35332–35347

intensity at 680 nm was due to electron/energy transfer and not simply due to introduction of a greater number of chloroplasts to the NPs, another experiment was designed. For this, PL enhancement was again studied for chlorophyll molecules with a gradual increase in NP concentration. It has been observed from the results (Figure 2e,f) that the emission peaks for chlorophyll treated with different concentrations of AgS and AgNPs were found to be intensified as compared with untreated chlorophyll. This holds true for all applied concentrations from 10 ppb to 100 ppm dosages of NPs. The substantial increase in the chlorophyll emission intensity on coupling with NPs was due to the antenna effect resulting from strong plasmonic interaction. Another observation also revealed that the augmentation in FL intensity was higher in AgS treatment compared to AgNP treatment. Based on this experimental outcome, the dosages for further in vitro light-dependent biochemical assays were determined.

Light-Dependent Reaction. In the light-dependent reaction, enhanced absorption of light energy is transformed into chemical energy. This in turn improves the electron transport rate, oxygen evolution rate, photophosphorylation activity, etc. The electronic band gap of these NPs allows them to convert the captured energy from the sun into excitons and also transfer electrons toward photosynthetic machinery. In our case, the high electron transfer from AgNPs and AgS to CLPs could possibly contribute to the formation of a stable CLP−NP complex. This brought the energy donor and acceptor molecules in close vicinity on the surface of CLPs and helped in formation of an in vitro hybrid light-harvesting complex. This association was more prominent in the case of AgS−CLP because of the overlapping absorption spectral pattern of NPs and CLP. To study the effect of such optically active engineered nanomaterials in ETC, we developed an in vitro CLP−NP hybrid photosynthetic model system. For different biochemical reactions, we have taken this model and different electron acceptor molecules to observe the rate of electron flow. It is well-established that plant chloroplasts release oxygen in the presence of ferricyanide, where the ferricyanide reduction occurs through electron transfer from PSII during the light-dependent reaction of photosynthesis.[32] It was depicted from the graph findings (Figure 3a) of ferricyanide reduction under appropriate light induction in the presence and absence of NPs, which was an indication of the energy transfer through electrons traveling down the line through the process.[23] Our study revealed that greater ferricyanide reduction took place in all AgNP- and AgS-treated samples with respect to the untreated control system. Maximum reduction was found at a dose of 100 ppm AgS, indicating 11.932 mM higher ferricyanide reduced/min with respect to the control. The results showed (Figure 3a) a gradual increase of ferricyanide reduction in the presence of NP treatment. In this case, the better efficacy resulted from the core/shell nanostructure. This confirmed a substantial amount of electron transfer and their entry into PSII in the presence of AgNPs and AgS, suggesting an augmented photoreduction of the electron acceptor. Oxygen evolution is a byproduct of the photosynthetic light reaction during oxidation of water molecules. Quantification of oxygen evolution as part of water splitting was thoroughly measured at this stage to relate it to the ETC activity. The oxygen evolution was measured polarographically[32] using DCPIP (2,6-dichlorophenolindophenol) as an artificial electron acceptor (Figure 3b). The highest oxygen evolution was found at a concentration of 1000 ppb for both AgNPs and AgS. At this dose, 1.9 and 3.6% increases in oxygen evolution were observed relative to control with AgNP and AgS treatment, respectively. Beyond this level, the amount of oxygen evolution for the AgNP−CLP cluster was at the same level as control sets, indicating the attainment of a saturation level. In the case of the AgS−CLP system, though the oxygen evolution was higher than that of control, it gradually reached the saturation level. This can be explained by the completion of the photoreduction, as all of the available electron acceptor molecules were already utilized.[33]

The Hill reaction, an alternate technique of polarography, was thoroughly investigated in terms of Hill activity measurement[30] utilizing the same electron acceptor, i.e., DCPIP (Figure 3c). The DCPIP decrease was proportional to the amount of oxygen generation throughout the electron transfer mechanism in photosynthesis. 29 and 34% reduction values of DCPIP were observed in comparison to control for the treatment concentrations of 100 ppm for AgNPs and AgS, respectively. As a result, the energy or electrons carried from NPs to CLP altered the whole PSII efficacy. The result corroborated our finding of oxygen evolution, where AgS showed better efficiency than AgNPs.

The very conventional process during light-dependent photosynthesis is electron transfer from PSII to PSI. A hole is naturally generated, as the electron stays at a higher energy level. This can result in a sprint of electrons downhill from PSII across multiple electron carriers to the PSI reaction center. To evaluate this pathway, the effects of AgNPs and AgS on PSI were also studied using NADP, another powerful electron acceptor molecule. The reduction of NADP to NADPH was accelerated in the presence of both NP treatments (Figure 3d), indicating a higher flow of electrons from PSII to PSI or straight from chlorophyll to PSI; this was also in agreement with the previously published report. In accordance with these observations, the reduction of NADP at all treatment concentrations of both AgNPs and AgS was higher with respect to control. As much as 164.3 and 198.86 mmol of excess NADPH was produced over an hour utilizing per mg of the leaf sample at the highest concentrations of AgNPs and AgS, respectively. Similarly, ferricyanide as an electron carrier was also a major indicator of the ETC process. The amount of reduced ferricyanide in the presence of treatment can directly indicate the entire ETC process of the cyclic pathway. This indicates the accumulation of more reduction power by the photosynthetic unit, and this could be utilized during the light-independent reaction of glucose formation.

The production of ATP was the final stage in the light cycle. Photophosphorylation is a way of transferring energy carried by a light-excited electron toward the pyrophosphate bond of an adenosine diphosphate (ADP) unit. It is one of the very important steps in noncyclic ETC, where ATP is produced to be utilized as a quantum of energy during a dark reaction. In this step, the released proton is routed to the ATPase unit via a proton gradient after water splitting to produce ATP. Figure 3e shows that the ATP content of AgNP- and AgS-treated chloroplast is higher than that of control. Between AgNPs and the core/shell nanostructure (AgS), the latter was found to perform better at 10 ppb, 100 ppb, 1000 ppb, 10 ppm, and 100 ppm concentrations. The percentage efficiency (17.7%) was highest in the 10 ppm AgS treatment. In a nutshell, when light fell on green tissues, these NPs encouraged the energy bundles found within the pigment layer to quickly transport electrons toward the reaction center, and these excess electrons were

https://doi.org/10.1021/acsomega.4c00550
ACS Omega 2024, 9, 35332−35347

never wasted. Both AgNPs and AgS improved chloroplast efficiency in the whole light-mediated electron transport pathway. The other associated biochemical reactions also showed how the transferred energy sharpened the subsequent electron transfer in light-dependent pathways, which caused greater ATP and NADPH5 generation and therefore enhanced the reducing potential generation during photosynthesis. This elevated PSII activity in the presence of AgNPs and AgS, with respect to the control condition, led to higher oxygen evolution. As an outcome, photophosphorylation activity was enhanced because of NP treatments. Both treatments therefore enhanced not only light absorption but also electron transfer throughout the complete light reaction, including cyclic and noncyclic ETC. A similar observation was also reported by Sharma et al.[34]

According to the findings of Rammler et al., a delocalized polaritonic state can be created between chlorophyll *a* molecules in the photosystems of living cells under ambient conditions in a microcavity,[35] and there should be generation of an electron−hole−photon (e−h−p) system within this microcavity as proposed by Horikiri et al. in semiconductor microcavities.[36] Wang et al. constructed a model integrating photosynthetic chlorophyll molecules on the nanostructured silver films.[37] They successfully showed that after absorbing photons, metal nanomaterials present in the proximity of photosynthetic chloroplast molecules generate LSPR, which increases the light-harvesting efficiency of the chlorophyll−nanoparticle complex. Moreover, this plasmonic nanostructure also generates DSPR, which can help in light entrapment at the interfaces. This model system showed increased light harvesting via the anti-Stokes process. This was facilitated by two simultaneous adsorptions: a low-energy photon and through the phonon mode of chlorophyll molecules.[38,39] So, the enhancement of light capture using a chlorophyll−nanometal conjugate can mainly be correlated with efficient excitation of excitons to an even higher level, contributed via the plasmon-induced enhancement of the local excitation field and exciton−phonon coupling in the anti-Stokes process.

Light-Independent Reaction. At the onset of the light-dependent cycle, apart from chlorophyll *a*, few antenna pigments also absorb solar irradiation and transfer the energy to PSI. Accumulation of a huge amount of energy makes the chloroplast unit highly excited, followed by dissipation of energy transfer. This phenomenon is known as the quenching of the excited state. This quenching was very much evident in all of the experiments carried out for studying cyclic and noncyclic ETC. In the light-independent reaction or dark cycle, CO_2 and water enzymatically combine with two 3C intermediates. These 3C compounds then undergo reduction in the presence of NADPH, generated during the light cycle, to produce carbohydrates. Our NP−CLP model system structures GPDHase and FDPase activities. When GPDHase (Figure 4a) and FBPase activities (Figure 4b) were measured in AgNP- and AgS-treated chloroplasts, it was found that both NPs were potent in increasing the activity of these two enzymes with respect to control. Surprisingly, with all NP concentration treatments, superior enzymatic activity was observed in both cases with respect to control. However, administration of dosages higher than 10 ppm showed a declining effect, which may be an indication of the saturating phase where reduction power was fully utilized for sugar formation. Second, as this experiment was carried out

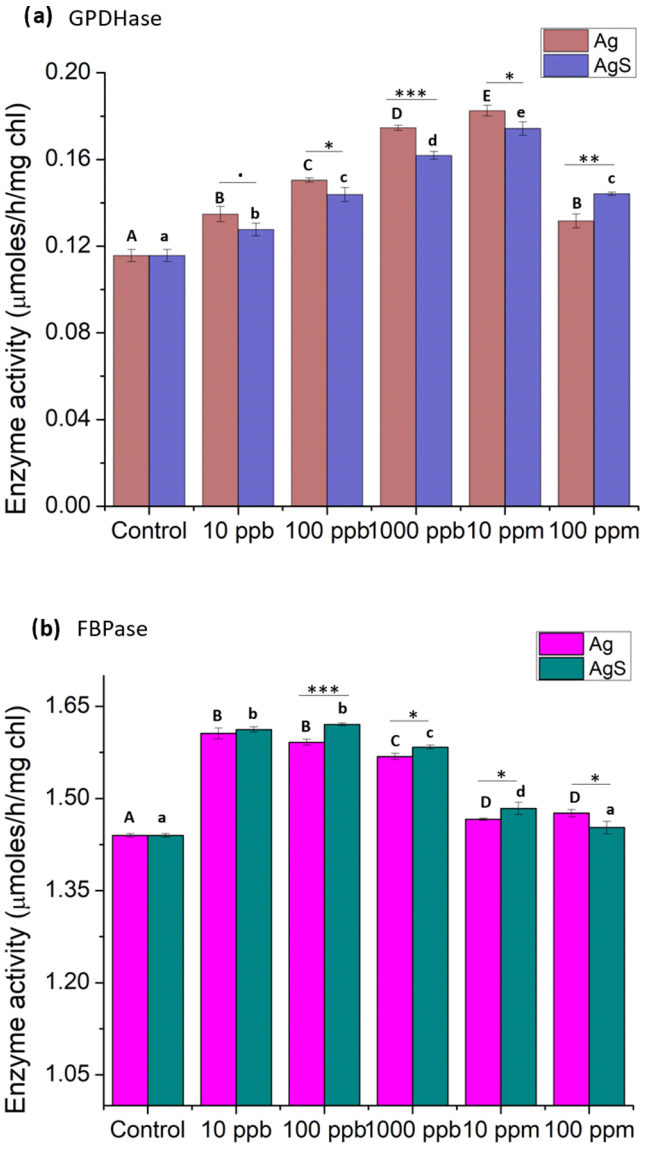

Figure 4. Changes in carbon assimilation in AgNP- and AgS-treated chloroplasts. (a) GPDHase activity [AgNP $F = 312.4$, $P < 0.001$; AgS $F = 207.9$, $P < 0.001$] and (b) FBPase activity [AgNP $F = 534.5$, $P < 0.001$; AgS $F = 488.7$, $P < 0.001$]. Within each type of treatment, mean data (±SE, $n = 3$) followed by the same uppercase letter are not significantly different for AgNP treatment, and those followed by the same lowercase letter are not significantly different for AgS treatment. (Tukey−Kramer HSD test). In each graph, symbols *, **, and *** denote $P < 0.05$, $P < 0.01$, and $P < 0.001$, respectively.

independent of light in vitro, the results obtained depicted the efficiency of NPs on the enzyme activity.

The augmented level of NADPH and ATP during in vitro light reactions in the presence of optically active NPs was not carried forward in this case, as this experiment was performed separately in the absence of light. So, the results clearly suggested that each AgNP and AgS might play a substantial role in the light-independent reaction as well, even without being photoinduced. This observation further claims that they expectedly impact more during natural plant growth conditions in a field where light and dark reactions are completely coherent in nature. Although our hypothesis mainly suggested and proved that optically active metallic and core/shell nanostructures can drive light absorption directly, this

https://doi.org/10.1021/acsomega.4c00550
ACS Omega 2024, 9, 35332−35347

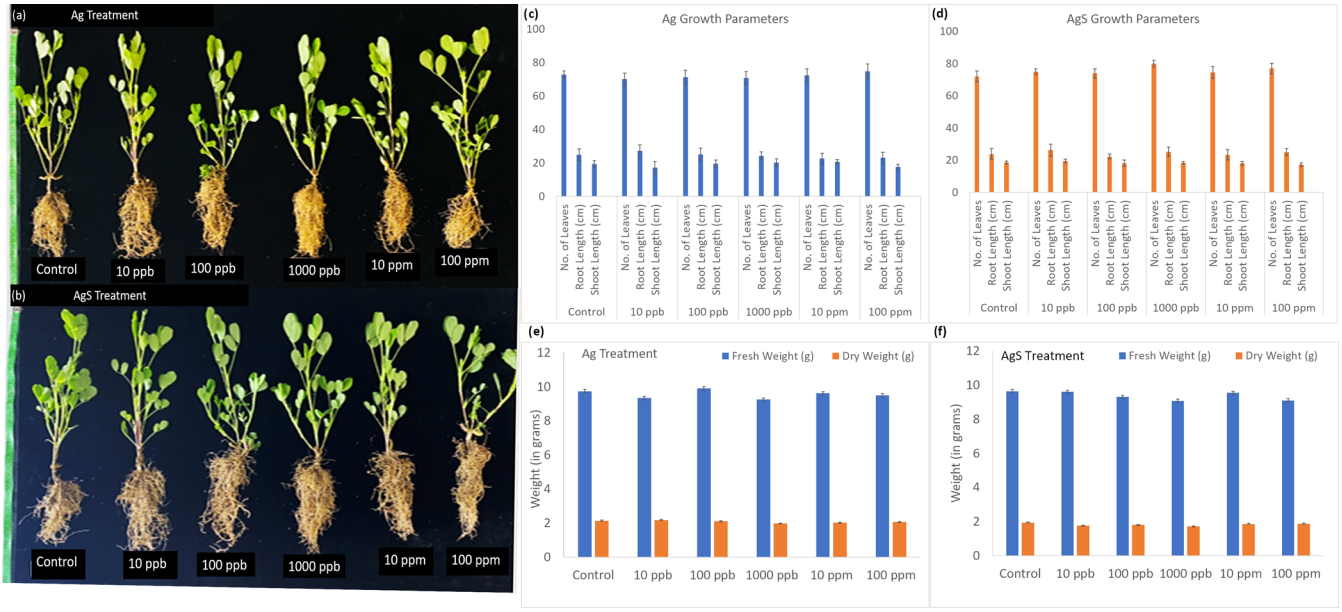

Figure 5. Morphology of control and AgNP- and AgS-treated *A. hypogaea* after 21 days. (a) Images of control and AgNP-treated plants. (b) Images of control and AgS-treated plants. No. of leaves, root length, and shoot length parameters of (c) control versus AgNP treatment and (d) control versus AgS treatment. Biomass comparison on treatment with (e) AgNPs and (f) AgS.

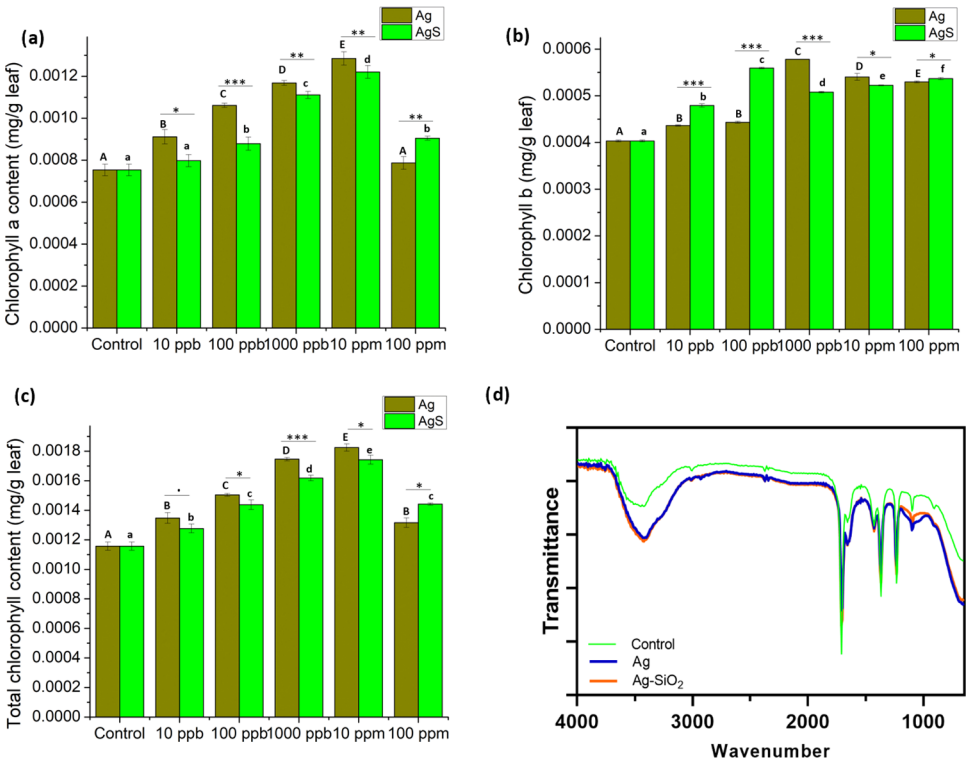

Figure 6. Effect of AgNPs and AgS on chlorophyll content of 21-day-treated *A. hypogaea* plants. (a) Chlorophyll *a* content [AgNP $F = 199.7$, $P < 0.001$; AgS $F = 155.6$, $P < 0.001$], (b) chlorophyll *b* content [AgNP $F = 1257$, $P < 0.001$; AgS $F = 2018$, $P < 0.001$], and (c) total chlorophyll content [AgNP $F = 312.4$, $P < 0.001$; AgS $F = 207.9$, $P < 0.001$]. Data represent the mean ± SE (n, no. of samples = 3) within each type of treatment. Mean data (±SE, $n = 3$) followed by the same uppercase letter are not significantly different for AgNP treatment, and those followed by the same lowercase letter are not significantly different for AgS treatment. (Tukey–Kramer HSD test). In each graph, symbols *, **, and *** denote $P < 0.05$, $P < 0.01$, and $P < 0.001$, respectively. (d) FTIR analysis showing the effect on the chlorophyll structure after treatment with AgNPs and AgS.

observation also revealed that they could positively induce a dark reaction.

Biosafety Study In Vivo. It is reported in several publications that nanomaterials may cause toxicity in plants, which can be characterized by metabolic disruptions and growth inhibition. To evaluate this phenomenon, we have carried out an in vivo analysis of plant growth parameters in the presence of AgNPs and AgS. Photographs of plants treated

https://doi.org/10.1021/acsomega.4c00550
ACS Omega 2024, 9, 35332−35347

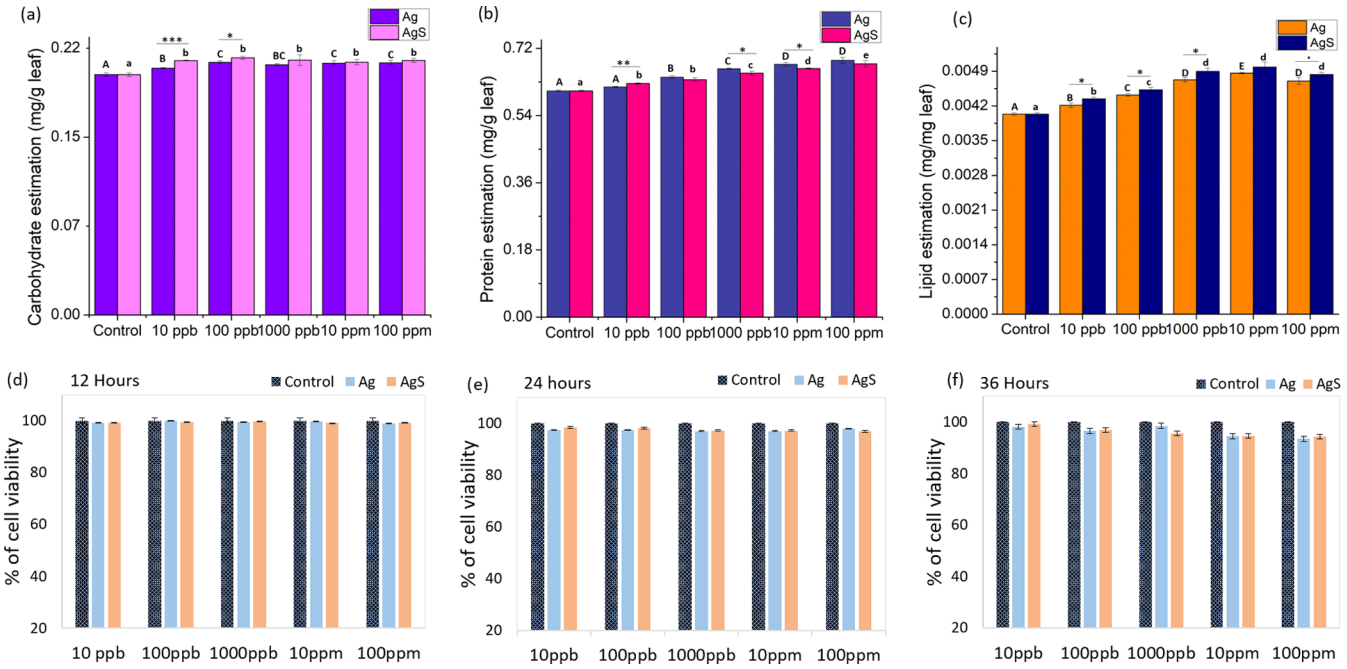

Figure 7. Quantification of (a) carbohydrate content [AgNP $F = 22$, $P < 0.001$; AgS $F = 14.7$, $P < 0.001$], (b) total protein content [AgNP $F = 192.2$, $P < 0.001$; AgS $F = 109.8$, $P < 0.001$], and (c) total lipid content [AgNP $F = 179.2$, $P < 0.001$; AgS $F = 120.5$, $P < 0.001$]. Within each type of treatment, mean data (±SE, $n = 3$) followed by the same uppercase letter are not significantly different for AgNP treatment, and those followed by the same lowercase letter are not significantly different for AgS treatment. (Tukey–Kramer HSD test). In each graph, symbols *, **, and *** denote $P < 0.05$, $P < 0.01$, and $P < 0.001$, respectively. The MTT assay rate of cell viability with respect to control on AgNP and AgS treatments after (d) 12 h, (e) 24 h, and (f) 36 h.

with NPs for 21 days with control sets are shown (Figure 5a,b). Treated plants were not found to exhibit any indication of stunted growth, abnormality in vigor, decline in the root structure, etc. Plants treated with AgNPs and AgS were found to be healthy at all dosages with no chlorotic or necrotic indications. As a result, no major abnormalities or stress responses were observed at any stage.

In the case of root length, the average length was almost the same with respect to control for all concentrations of AgNPs and AgS (Figure 5c,d). The plants were healthy even for the treatment at the highest concentration of 100 ppm. A similar pattern of data was also observed in the case of shoot length and leaf count as well, where the overall effect of both NPs seemed to be nontoxic.

Total biomass in plants is closely related to plant growth and is a direct outcome of photosynthetic capability, environmental conditions, nutrition, and other aspects. Although the fresh weights of control and treated plants differed slightly (but not significantly), the dry weight was nearly identical (Figure 5e,f). The dry weight represents the total amount of inorganic and organic substances in the plant tissue. Since dry weight measures biomass precisely, it eliminates fluctuations caused by water content. In our experiment, for different NP dosages, the dry weight was almost like control, indicating no detrimental impact on growth parameters.

Another significant characteristic to consider when examining the key physiological process of photosynthesis is the chloroplast pigment concentration. Nanomaterials are well known to increase chlorophyll content in plants, although the effect may vary with plant species and target nanomaterials. Rad et al. reported that SiO_2 NPs increased chlorophyll *a* and *b* and carotenoid content in treated plants.[40] ZnO NPs were reported to improve seed germination, seedling vigor, flowering, and leaf chlorophyll content.[41] Ghafari and Razmjoo found enhancement in chlorophyll content and antioxidant enzyme activity when wheat plants were treated with FeO NPs.[42] Mohamed et al. discovered that priming with lower concentrations of AgNPs increased total chlorophyll content, whereas higher concentrations of AgNPs and SiO_2 NPs decreased it.[43,44]

In our study, chlorophyll *a* content was found to be increased at concentrations until 10 and 100 ppm concentrations of AgNP and AgS treatment, respectively (Figure 6a). In comparison with control, NP treatments showed a similar rise in chlorophyll *b* and total chlorophyll content (Figure 6) with respect to control. Because chlorophyll *a* and *b* both absorb photoirradiation from 430 to 660 nm, a rise in their quantity indicates an increase in the efficiency of photosynthetic activity. In our bioassays, both AgNP and AgS treatments resulted in the overall enhancement of total chlorophyll content with respect to control (Figure 6c). The marginal difference between the two nanostructures in contributing to pigment content can probably be explained by the effect of the silica shell over AgNPs. SiO_2 NPs have also been reported to show a positive effect on the photosynthetic rate and stomatal conductance with no effect on chlorophyll and carotenoid content of Crataegus sp.[45] This finding corroborates our result, where the SiO_2 shell improved the optoelectronic property of metal nanostructures and photosynthetic efficiency with a significant increase in pigment content. This can be justified as Xie et al. showed SiO_2 NPs to be accelerating photosynthesis by increasing carbonic anhydrase activity and photosynthetic pigment contents.[46] These results can be varied from species to species.

FTIR Measurement of Chlorophyll–NP Conjugates. The experiment was designed to study any change in the

https://doi.org/10.1021/acsomega.4c00550
ACS Omega 2024, 9, 35332−35347

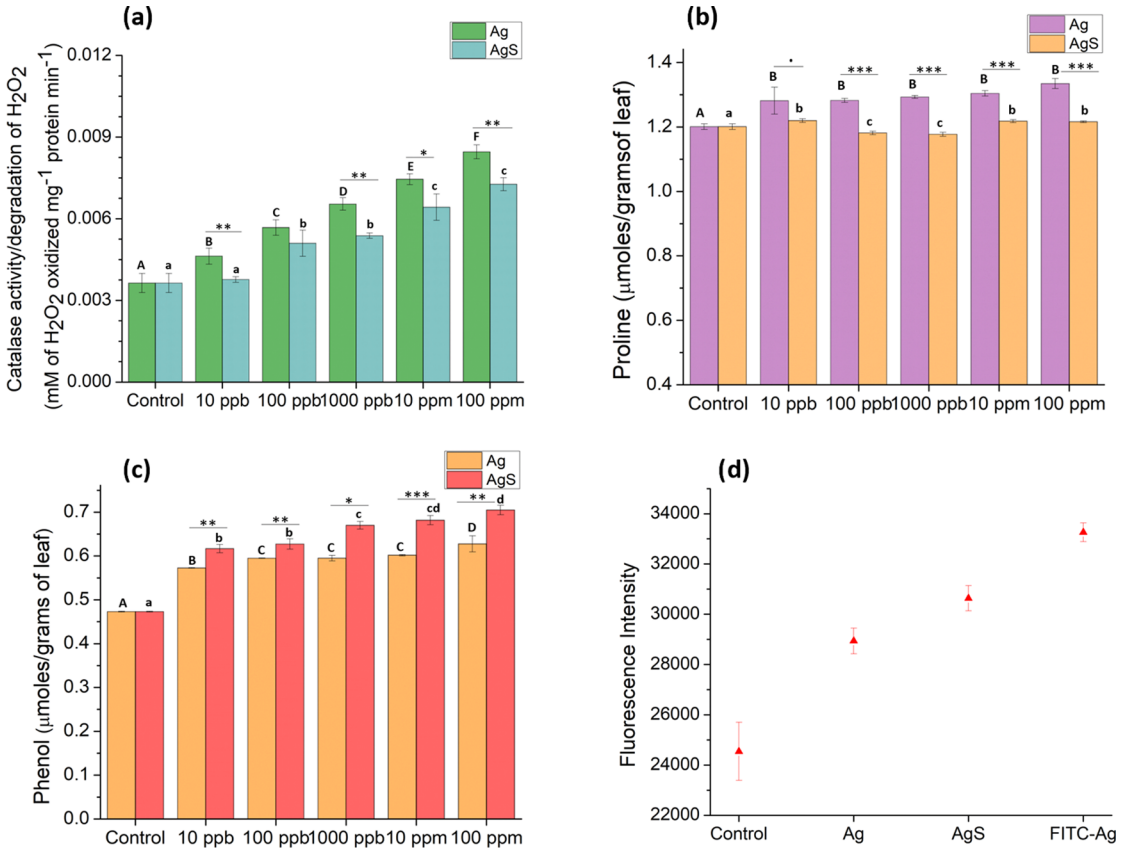

Figure 8. Effect on (a) catalase activity [AgNP $F = 128.9$, $P < 0.001$; AgS $F = 55.27$, $P < 0.001$], (b) proline content [AgNP $F = 16.3$, $P < 0.001$; AgS $F = 31.98$, $P < 0.001$], and (c) phenol content [AgNP $F = 137$, $P < 0.001$; AgS $F = 233.5$, $P < 0.001$] of AgNP- and AgS-treated *A. hypogaea* plants after 21 days. Data represent mean ± SE (n, no. of samples = 3) within each type of treatment; mean data (±SE, $n = 3$) followed by the same uppercase letter are not significantly different for AgNP treatment, and those followed by the same lowercase letter are not significantly different for AgS treatment. (Tukey–Kramer HSD test). In each graph, symbols *, **, and *** denote $P < 0.05$, $P < 0.01$, and $P < 0.001$, respectively. (d) Fluorescence intensity correlation graph among control, AgNPs, AgS, and FITC-tagged AgNP treatment sets of chlorophyll extracted from in vivo-treated *A. hypogaea*. Within the graph, each type of treatment represents mean data (±SE, $n = 3$).

structure of chlorophyll with NP treatment. The extracted chlorophyll as the control set and two treatment sets with AgNPs and AgS were analyzed with FTIR. No change in vibrational energy or any functional group peak could be observed from the graph (Figure 6d), showing no alterations in the chlorophyll structure. Moreover, no additional peak for AgS was obtained, as the peak of chlorophyll aligned with that of AgS at 1073 cm^{-1}.

Quantification of Carbohydrate, Protein, and Lipid Content. NPs have unique features due to their higher surface area-to-volume ratio, presence of a higher number of surface electrons, increased catalytic properties, enhanced optoelectronic functionalities, etc. The higher concentrations of AgNPs were reported to be toxic to plants.[47,48] For the successful application of this novel technology in a broad spectrum, it was very important to study the toxicity profile of proposed nanostructures. From our bioassay, increases in total carbohydrate (Figure 7a), protein (Figure 7b), and lipid (Figure 7c) content were evident in treatment with respect to control sets. An increase in sugar content can directly be correlated with the higher photosynthetic rate in the presence of NPs. Starting from the very low dose (10 ppb) to the highest amount, the applied sugar content was found to be augmented in all treatments. In the case of the total protein content (Figure 7b), a gradual increase was observed with increasing concentrations of NP treatment. For the lipid content (Figure 7c), the highest amount of lipid was obtained with the treatment at 10 ppm. Hence, it may be concluded that both AgNP and AgS treatments have underscored the biosafety concern in the plant model system.

Increased photosynthesis is generally correlated with improved growth parameters. The obtained result indicated that NP treatments can induce a more beneficial effect on the primary plant growth parameter. However, it was not observed for all of the parameters like root length, shoot length, etc. Since these plants were grown within artificial and limited conditions, this may not totally reflect the ideal field situation. Moreover, previous studies also revealed that an almost 30% increase in plant photosynthesis could only contribute to 2–4% of plant growth.[49]

Photosynthesis is the sole source of food production in plants, but plant growth and vigor are complex attributes depending upon numerous factors. These include utilization of available nutrients, phase of growth, environmental conditions, seasonal variation, disease defense mechanism, etc. This study provides an impetus to further examine the effect of these nanostructures at the field level to get a clearer picture of growth and other aspects of plant development.

MTT Toxicity Analysis. As the exposure of AgNPs to humans and plants advances, a substantial volume of experimental evidence of severe/acute cytotoxicity produced by AgNPs has prompted serious concerns and discussions over

https://doi.org/10.1021/acsomega.4c00550
ACS Omega 2024, 9, 35332–35347

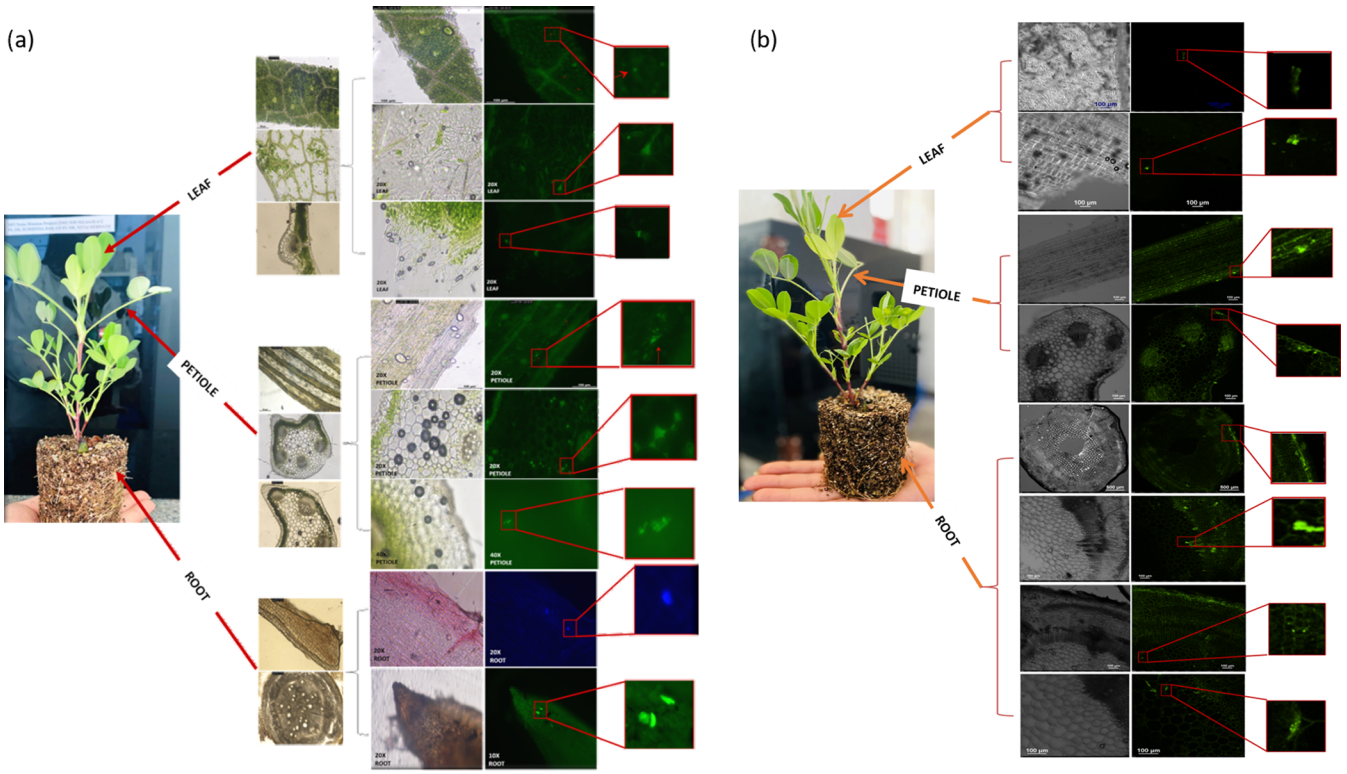

Figure 9. Microscopic images of hand-sectioned different parts of *A. hypogaea* after 24 h of treatment with FITC-tagged AgNPs. (a) Fluorescence microscopic images and (b) confocal microscopic images from three different tissues. The microscopic images show the translocation of FITC-tagged AgNPs within *A. hypogaea* plants. The plants were grown in a controlled environment prior to treatment.

their safety.[50] To address this concern of toxicity toward exposed organisms, an MTT assay was conducted for cell viability studies in the MDA-MB-231 (human breast cancer) cell line.

The results were compared with control sets after 12 h (Figure 7d), 24 h (Figure 7e), and 36 h (Figure 7f) exposure time. All of the treatments showed nearly 90% cell viability even after treatment with the highest concentration (100 ppm) of AgNPs and AgS. A Mini Review article by Mishra and Singh revealed that silver-based NPs can be utilized in permissible limits in agri-ecosystems as an advanced agriproduct.[51] Many other studies reported toxic effects of silver ions released from AgNPs, showing toxic effects on cells, which included adverse effects on the cell cycle,[52] causing cell apoptosis via oxidative damage.[53−56] Ernst et al. observed silver accumulation in the rat kidney after a single intravenous injection of radiolabeled $AgNO_3$ containing 0.5 mg of Ag per rat.[57] Tiwari et al. examined the dose-related in vivo toxicity of silver in Wistar rats. Four different AgNP doses (4, 10, 20, and 40 mg/kg) were administered intravenously.[58] In the past, it was also shown that the discharged Ag^+ produced fibroblast cell membrane disruption and triggered cell death.[59] Although we did not find our nanomaterials to be toxic to the cell line and plant model system, further detailed acute toxicity studies in other model systems are required before their successful application at the field level.

ROS Assay of Nanomaterial-Treated Plants. Photosynthesis is highly susceptible to changes in light,[60] and with continuous exposure to UV-B radiation, it causes excessive accumulation of ROS in plant chloroplasts, which damages PSII and decreases the electron transfer rate and thylakoid membrane stability.[61] Despite their damaging nature, ROS are a well-known second messenger in a range of cellular activities, including stress tolerance.[62−64] The fragile equilibrium between ROS generation and ROS scavenging determines whether ROS will operate as damaging or signaling molecules. Because of the multifaceted functions of ROS, cells need strict management over the quantity of ROS to minimize oxidative harm but not eliminate them. NPs play an essential role in plant defense against a variety of abiotic challenges[65] by activating antioxidative enzymes that scavenge ROS produced by abiotic stressors.[66,67] However, various plant species respond differently to NPs.[68] Excess ROS are scavenged or detoxified by an effective antioxidative system involving both nonenzymic and enzymic antioxidants.[69] Plant growth and development are impeded by ROS levels that are either low or too high, whereas retaining ROS levels in the acceptable range supports plant health.[70]

In our experimental studies, the catalase activity is found to be increased in both AgNP and AgS treatments (Figure 8a). Catalase detoxifies the plant by turning H_2O_2 into water and oxygen. Catalase activity in plants was increased at concentrations from 10 ppb to 100 ppm for AgNP treatment in contrast with control. In AgS treatment, other than 10 ppb concentration dose-dependent increase in catalase activity was observed. Both AgNP and AgS treatments appeared to have stimulated the enzyme to scavenge more H_2O_2. Several researchers have also observed increased levels of antioxidant defense response enzymes in plants to counteract oxidative stress caused by varied environmental stress. Plants' resilience to such environmental stressors has been associated with maintaining a strong antioxidant ability to scavenge harmful ROS.[71,72] Undoubtedly, changes in ROS levels that are part of the plant's inherent metabolism should not surpass the

https://doi.org/10.1021/acsomega.4c00550
ACS Omega 2024, 9, 35332−35347

threshold between redox biology and cytostatic or cytotoxic levels.[70] In our studies, the ROS level did not seem to have increased to such levels (as observed from the primary growth data obtained from in vivo bioassays). Neither of the treatments showed any detrimental effect on plant health despite increased catalase activity.

Nonantioxidative protein components such as proline (Figure 8b) and phenol (Figure 8c) contents were also determined. Plants have general strategies to induce the activities of these nonantioxidative proteins to overcome oxidative stress due to imposition of abiotic stress. Phenolic compounds act as electron donors, as the hydroxyl groups they contain may directly aid in free radical scavenging.[73] Furthermore, some of them stimulate the synthesis of endogenous antioxidant molecules in the cell.[74] Plant phenol production may increase in response to abiotic stresses like severe weather, exposure to heavy metals, salt, and radiation as well.[75] In our experimental observations, the amount of phenol was increased in both AgNP and AgS treatments for concentrations up to 100 ppm with respect to control (Figure 8c). These phenolic compounds may increase as a response to higher ROS generation, which could be due to higher photosynthetic activity, as explained earlier. Plants may produce phenols as a tolerance response to cope with unfavorable conditions under abiotic stress.[76] In literature also, it is reported that NPs can improve plants' resistance to abiotic stressors by increasing the phenol level, but the mechanism behind this inhibition is not clear yet.[5] So, a change in the phenol level in our results could be attributed to the plant defense strategy.

Proline content on the other hand is recognized to be an indicator of stress in plants, which could act as an osmoprotectant, and increased proline accumulation would prevent membrane deformation by scavenging hydroxyl radicals.[33] Several studies attribute an antioxidant property to proline, suggesting ROS scavenging activity and acting as a singlet oxygen quencher.[62] Proline is an excellent index of the existing stress experienced by plants, since the proline level declines after relief from stress.[77] This could explain the decreased levels of proline content in the case of AgS treatment (Figure 8b). An unprecedented decline in proline levels recorded in the present experiments is one of the most convincing pieces of evidence for improved electron exchange efficiency in AgS-treated plants. It follows that the optimized use of AgS can modulate oxidative stress in plants.

Translocation of Nanomaterials in the Plant System. To understand the bioavailability of AgNPs, the presence of fluorescently labeled AgNPs (AgNP-FITC) was studied by fluorescence and confocal microscopy. Bright green fluorescence was observed under an FITC filter in samples indicative of FITC-tagged AgNPs within the treated leaf, petiole, and root specimens (Figure 9a). Blue fluorescence could also be seen under a DAPI filter after treatment with AgNPs, since the NPs were themselves fluorescent. Similarly, following the same procedure, confocal images were also taken with FITC-AgNPs (Figure 9b).

Because of the ultrasmall size, it was difficult to locate NPs in a bright-field microscope. Although thorough sonication of these AgNPs was performed before application, agglomeration was still evident. This in turn facilitated the identification of NPs upon excitation during fluorescence and confocal microscopy. Hence, focusing on the localized NP clusters could reveal the presence of nanomaterials in the cross sections of treated plant parts. These data clearly represented that plants treated with fluorescent NPs exhibited the presence of NPs at the exact area of application (root), and a significant amount of these particles was also translocated in different tissues of plants like petiole, leaf, etc. Xylem vesicles of petiole and leaf sections also showed the presence of fluorescence signals in considerable amounts. A similar kind of translocation study by Zhu et al. also exhibited the presence of NPs in different plant parts.[78]

Ag^+ Release Study by ICP-MS. After the translocation of FITC-tagged AgNPs, ICP-MS was performed to measure biodistribution of Ag from AgNP at trace levels in *A. hypogaea*. After the standard ICP procedure and calibration against the Ag standard, we found that 438.12 μg/kg Ag was present within the AgS-treated plant sample. The in vivo presence of AgNPs was evident from the results, which also corroborated the data of translocation studies. This also indirectly indicated that NPs were carried by the leaves of the plant samples, which later interacted with the chloroplast responsible for augmented photosynthesis.

Chloroplast Fluorescence Intensity Measurement. Photoinhibition is a phenomenon that causes a decrease in photosynthetic activity, primarily because of the light-induced decrease in CO_2 assimilation.[79,80] Even though the reduction in photoassimilation may be due to the damage to various components of the photosynthetic machinery, the concept of photoinhibition is widely used to denote light-induced inhibition of PSII activity.[81−83] Our experiment was designed to study the change in the fluorescence intensity of chloroplasts in in vivo treatment. The results showed an increase in chlorophyll fluorescence intensity when treated with AgNPs, AgS, and FITC-tagged AgNPs, indicating no photoinhibition (Figure 8d). Photoinhibition is unavoidable when light surpasses the photosynthetic rate, since light is the energy required to drive the photosynthetic process.[79] There is a higher difference in FL intensity, as the NPs under investigation are self-fluorescent (Figure S1 in the SI section) in nature. Since the results were obtained in the in vivo system, the fluorescence nature of NPs did not change much, and the enhanced fluorescence results can be related to a higher photosynthetic rate.

CONCLUSIONS

The study provides a detailed account of the effect of NPs on light acquisition and other photosynthetic parameters in a plant model system. In all of the light-dependent photosynthetic reactions, incorporation of the nanostructures showed an enhancement in the end products. In vitro light-independent reactions also revealed an increase in key light-independent enzyme activity. In vitro and in vivo translocation assays of the FITC-tagged NPs confirmed the presence of NPs in the plant model system. A detailed toxicity analysis of these nanomaterials in a plant model and an animal cell line did not exhibit any detrimental effect. It was apparent that because of the silica shell, the light-harvesting property was better in the case of AgS, and this also helped in masking the oxidative stress caused by AgNP treatment alone. Finally, analyses of all of the biochemical parameters confirmed that higher electron transfer was correlated with overall photosynthetic efficiency. Further investigations are required to correlate the augmentation of photosynthetic efficiency with other plant metabolic pathways, which can lead to more flowering and fruiting and enhanced disease management. To the best of our knowledge, this study

https://doi.org/10.1021/acsomega.4c00550
ACS Omega 2024, 9, 35332−35347

is the first experimental proof to show the effect of overlapping photoluminescence properties of chloroplasts and NPs, modulating the photosynthesis process in vitro. These detailed experimental analyses may have two definite future directions. Primarily, this study will provide a positive impetus to metal and core/shell metal-based nanostructures in developing CLP−NP-based artificial photosynthetic machinery. A detailed chronic toxicity analysis will be required for agricultural applications. This study may further open the possibility for the development of plant-based nanobionic devices for various other applications like communication, energy harvesting, environment sensing, solar system, conversion, etc. This modern approach also has the capacity to bypass the complexity of myriad plastic boards containing circuits that consume power from electrical grids.

■ ASSOCIATED CONTENT

Supporting Information

The Supporting Information is available free of charge at https://pubs.acs.org/doi/10.1021/acsomega.4c00550.

Protocol for physicochemical characterization of nanoparticles; methodologies to carry out the toxicity assays in the plant model system and the human breast cancer cell line; Figure S1 represents the fluorescence microscopy images of AgNPs; and Table S1 shows time-dependent stability of AgS and AgNPs based on DLS analysis (PDF)

■ AUTHOR INFORMATION

Corresponding Author

Sumistha Das − *Amity Institute of Biotechnology, Amity University Haryana, Gurugram 122413, India;* orcid.org/0009-0007-6754-3922; Email: sumistha.das@gmail.com

Authors

Shikha Dhiman − *Amity Institute of Biotechnology, Amity University Haryana, Gurugram 122413, India*

Nitai Debnath − *Amity Institute of Biotechnology, Amity University Haryana, Gurugram 122413, India;* orcid.org/0000-0001-5930-4402

Kaustav Bandyopadhyay − *Amity Institute of Biotechnology, Amity University Haryana, Gurugram 122413, India*

Complete contact information is available at: https://pubs.acs.org/10.1021/acsomega.4c00550

Funding

Department of Science & Technology, Govt. of India, (DST) Grant Nos YSS/2015/000152 and DST/NM/NS/2018/27 for providing financial support.

Notes

The authors declare no competing financial interest.

■ ACKNOWLEDGMENTS

The authors are grateful to the Department of Science & Technology, Govt. of India, (DST) Grant Nos. YSS/2015/000152, DST/NM/NS/2018/27, CRG/2022/002730, and BT/INF/22/SP45072/2022 for providing financial support. The authors are very much thankful to the National Institute of Plant Genome Research (NIPGR), Department of Biotechnology, Govt. of India, for providing seeds for our study. The authors are grateful to Dr. Ashish Ranjan from NIPGR for all his guidance. The authors would like to acknowledge Dr. Amit Kumar Pandey and Bhupender Yadav for helping with cell viability assays. The authors would also like to acknowledge the Central Instrumentation Research Facility (CIRF), Amity University Haryana, for instrumentation facilities and infrastructural support.

■ REFERENCES

(1) Nealson, K. H.; Conrad, P. G. Life: Past, present and future. *Philos. Trans. R. Soc. London* **1999**, *354* (1392), 1923−1939.

(2) Weise, S. E.; Weber, A. P.; Sharkey, T. D. Maltose is the major form of carbon exported from the chloroplast at night. *Planta* **2004**, *218* (3), 474−482.

(3) Zhu, X.-G.; Long, S. P.; Ort, D. R. Improving photosynthetic efficiency for greater yield. *Annu. Rev. Plant Biol.* **2010**, *61* (1), 235−261.

(4) Blankenship, R. E.; Tiede, D. M.; Barber, J.; Brudvig, G. W.; Fleming, G.; Ghirardi, M.; Gunner, M. R.; Junge, W.; Kramer, D. M.; Melis, A.; Moore, T. A.; Moser, C. C.; Nocera, D. G.; Nozik, A. J.; Ort, D. R.; Parson, W. W.; Prince, R. C.; Sayre, R. T. Comparing photosynthetic and photovoltaic efficiencies and recognizing the potential for improvement. *Science* **2011**, *332* (6031), 805−809.

(5) Kataria, S.; Jain, M.; Rastogi, A.; Živčák, M.; Brestic, M.; Liu, S.; Tripathi, D. K. Role of nanoparticles on photosynthesis. *Nanomater. Plants, Algae, Microorg.* **2019**, 103−127.

(6) Giraldo, J. P.; Landry, M. P.; Faltermeier, S. M.; McNicholas, T. P.; Iverson, N. M.; Boghossian, A. A.; Reuel, N. F.; Hilmer, A. J.; Sen, F.; Brew, J. A.; Strano, M. S. Plant nanobionics approach to augment photosynthesis and biochemical sensing. *Nat. Mater.* **2014**, *13* (4), 400−408.

(7) Wilhelm, C.; Selmar, D. Energy dissipation is an essential mechanism to sustain the viability of plants: The physiological limits of improved photosynthesis. *J. Plant Physiol.* **2011**, *168* (2), 79−87.

(8) Scholes, G. D.; Fleming, G. R.; Olaya-Castro, A.; Van Grondelle, R. Lessons from nature about solar light harvesting. *Nat. Chem.* **2011**, *3* (10), 763−774.

(9) Chandra, S.; Pradhan, S.; Mitra, S.; Patra, P.; Bhattacharya, A.; Pramanik, P.; Goswami, A. High throughput electron transfer from carbon dots to chloroplast: A rationale of enhanced photosynthesis. *Nanoscale* **2014**, *6* (7), 3647−3655.

(10) Cossins, D. Next generation: Nanoparticles augment plant functions. The incorporation of synthetic nanoparticles into plants can enhance photosynthesis and transform leaves into biochemical sensors. The Scientist, News & Opinion. March 16, 2014. https://www.the-scientist.com/daily-news/next-generation-nanoparticles-augment-plant-functions-37804.

(11) Govorov, A. O.; Carmeli, I. Hybrid structures composed of photosynthetic system and metal Nanoparticles: Plasmon enhancement effect. *Nano Lett.* **2007**, *7* (3), 620−625.

(12) Dhiman, S.; Yadav, A.; Debnath, N.; Das, S. Application of core/Shell nanoparticles in smart farming: A paradigm shift for making the agriculture sector more sustainable. *J. Agric. Food Chem.* **2021**, *69* (11), 3267−3283.

(13) Ghosh Chaudhuri, R.; Paria, S. Core/Shell nanoparticles: Classes, properties, synthesis mechanisms, characterization, and applications. *Chem. Rev.* **2012**, *112* (4), 2373−2433.

(14) Negishi, R.; Naya, S.; Kobayashi, H.; Tada, H. Gold(core)-lead(shell) nanoparticle-loaded Titanium(IV) oxide prepared by Underpotential Photodeposition: Plasmonic water oxidation. *Angew. Chem.* **2017**, *129* (35), 10483−10487.

(15) Cao, Z.; Stowers, C.; Rossi, L.; Zhang, W.; Lombardini, L.; Ma, X. Physiological effects of cerium oxide nanoparticles on the photosynthesis and water use efficiency of soybean (Glycine Max (L.) Merr.). *Environ. Sci.: Nano* **2017**, *4* (5), 1086−1094.

(16) Zhang, G.; Lan, Z.; Lin, L.; Lin, S.; Wang, X. Overall water splitting by Pt/G-$c_3N_4$photocatalysts without using sacrificial agents. *Chem. Sci.* **2016**, *7* (5), 3062−3066.

(17) Zheng, D.; Cao, X.; Wang, X. Precise formation of a hollow carbon nitride structure with a Janus surface to promote water

splitting by Photoredox catalysis. *Angew. Chem., Int. Ed.* **2016**, *55* (38), 11512−11516.
(18) Li, Y.; Kong, T.; Shen, S. Artificial photosynthesis with polymeric carbon nitride: When meeting metal nanoparticles, single atoms, and molecular complexes. *Small* **2019**, *15* (32), No. 1900772.
(19) Noji, T.; Kamidaki, C.; Kawakami, K.; Shen, J.; Kajino, T.; Fukushima, Y.; Sekitoh, T.; Itoh, S. Photosynthetic oxygen evolution in Mesoporous silica material: Adsorption of Photosystem II reaction center complex into 23 nm Nanopores in SBA. *Langmuir* **2011**, *27* (2), 705−713.
(20) Zhang, B.; Zheng, L. P.; Yi Li, W.; Wen Wang, J. Stimulation of Artemisinin production in artemisia annua hairy roots by ag-sio2 core-shell nanoparticles. *Curr. Nanosci.* **2013**, *9* (3), 363−370.
(21) Radziuk, D.; Skirtach, A.; Sukhorukov, G.; Shchukin, D.; Möhwald, H. Stabilization of Silver Nanoparticles by Polyelectrolytes and Poly(ethylene glycol). *Macromol. Rapid Commun.* **2007**, *28* (7), 848−855.
(22) Thakur, S.; Kumar, P.; Reddy, M. V.; Siddavattam, D.; Paul, A. Enhancement in sensitivity of fluorescence based assay for organophosphates detection by silica coated silver nanoparticles using organophosphate hydrolase. *Sens. Actuators, B* **2013**, *178*, 458−464.
(23) Gerwick, B. C.; Williams, G. J.; Uribe, E. G. Effects of temperature on the hill reaction and Photophosphorylation in isolated cactus chloroplasts. *Plant Physiol.* **1977**, *60* (3), 430−432.
(24) Vishniac, W. [15] methods for study of the hill reaction. *Methods Enzymol.* **1957**, *4*, 342−355.
(25) Terry, N.; Huston, R. P. Effects of calcium on the photosynthesis of intact leaves and isolated chloroplasts of sugar beets. *Plant Physiol.* **1975**, *55* (5), 923−927.
(26) Wang, P.; Duan, W.; Takabayashi, A.; Endo, T.; Shikanai, T.; Ye, J.; Mi, H. Chloroplastic NAD(P)H Dehydrogenase in tobacco leaves functions in alleviation of oxidative damage caused by temperature stress. *Plant Physiol.* **2006**, *141* (2), 465−474.
(27) Tripathy, B. C.; Mohanty, P. Zinc-inhibited electron transport of photosynthesis in isolated Barley chloroplasts. *Plant Physiol.* **1980**, *66* (6), 1174−1178.
(28) Taylor, S. E.; Terry, N.; Huston, R. P. Limiting factors in photosynthesis. *Plant Physiol.* **1982**, *70* (5), 1541−1543.
(29) Goodwin, T. W. (Ed.). *Chemistry and biochemistry of plant pigments*, 1976.
(30) Valeur, B.; Berberan-Santos, M. N. A brief history of fluorescence and phosphorescence before the emergence of quantum theory. *J. Chem. Educ.* **2011**, *88* (6), 731−738.
(31) Breton, J. The 695 nm fluorescence (F_{695}) of chloroplasts at low temperature is emitted from the primary acceptor of photosystem II. *FEBS Lett.* **1982**, *147* (1), 16−20.
(32) Barr, R.; Crane, F. L. Ferricyanide reduction in Photosystem II of spinach chloroplasts. *Plant Physiol.* **1981**, *67* (6), 1190−1194.
(33) Pradhan, S.; Patra, P.; Das, S.; Chandra, S.; Mitra, S.; Dey, K. K.; Akbar, S.; Palit, P.; Goswami, A. Photochemical modulation of Biosafe manganese nanoparticles on *Vigna radiata*: A detailed molecular, biochemical, and biophysical study. *Environ. Sci. Technol.* **2013**, *47* (22), 13122−13131.
(34) Sharma, P.; Bhatt, D.; Zaidi, M. G.; Saradhi, P. P.; Khanna, P. K.; Arora, S. Silver nanoparticle-mediated enhancement in growth and antioxidant status of brassica juncea. *Appl. Biochem. Biotechnol.* **2012**, *167* (8), 2225−2233.
(35) Rammler, T.; Wackenhut, F.; Zur Oven-Krockhaus, S.; Rapp, J.; Forchhammer, K.; Harter, K.; Meixner, A. J. Strong coupling between an optical microcavity and photosystems in single living cyanobacteria. *J. Biophotonics* **2021**, *15* (2), No. e202100136, DOI: 10.1002/jbio.202100136.
(36) Horikiri, T.; Byrnes, T.; Kusudo, K.; Ishida, N.; Matsuo, Y.; Shikano, Y.; Löffler, A.; Höfling, S.; Forchel, A.; Yamamoto, Y. Highly excited exciton-polariton condensates. *Phys. Rev. B* **2017**, *95* (24), No. 245122, DOI: 10.1103/PhysRevB.95.245122.
(37) Wang, Y.-L.; Nan, F.; Liu, X.; Zhou, L.; Peng, X.; Zhou, Z.; Yu, Y.; Hao, Z.; Wu, Y.; Zhang, W.; Wang, Q.; Zhang, Z. Plasmon-enhanced light harvesting of chlorophylls on near-percolating silver films via one-photon Anti-Stokes Upconversion. *Sci. Rep.* **2013**, *3* (1), No. 1861, DOI: 10.1038/srep01861.
(38) Mackowski, S.; Wörmke, S.; Maier, A. J.; Brotosudarmo, T. H.; Harutyunyan, H.; Hartschuh, A.; Govorov, A. O.; Scheer, H.; Bräuchle, C. Metal-enhanced fluorescence of chlorophylls in single light-harvesting complexes. *Nano Lett.* **2008**, *8* (2), 558−564.
(39) Drachev, V.; Kim, W. T.; Safonov, V.; Podolskiy, V.; Zakovryashin, N.; Khaliullin, E.; Shalaev, V.; Armstrong, R. Low-threshold lasing and broad-band multiphoton-excited light emission from Ag aggregate-adsorbate complexes in microcavity. *J. Mod. Opt.* **2002**, *49* (3−4), 645−662, DOI: 10.1080/09500340110087246.
(40) Rad, J. S.; Karimi, J.; Mohsenzadeh, S.; Rad, M. S.; Moradgohli, J. Evaluation SiO2 Nanoparticles Effects on Developmental Characteristic and Photosynthetic Pigment Contents of Zea mays L. *Bull. Environ., Pharmacol. Life Sci.* **2014**, *3*, 194−201.
(41) Prasad, T. N. V. K. V.; Sudhakar, P.; Sreenivasulu, Y.; Latha, P.; Munaswamy, V.; Reddy, K. R.; Sreeprasad, T. S.; Sajanlal, P. R.; Pradeep, T. Effect of nanoscale zinc oxide particles on the germination, growth and yield of peanut. *J. Plant Nutr.* **2012**, *35* (6), 905−927.
(42) Ghafari, H.; Razmjoo, J. Effect of foliar application of nano-iron oxidase, iron chelate and iron sulphate rates on yield and quality of wheat. *Int. J. Agron. Plant Prod.* **2013**, *11* (4), 2997−3003.
(43) Mohamed, A. K. S. H.; Qayyum, M. F.; Abdel-Hadi, A. M.; Rehman, R. A.; Ali, S.; Rizwan, M. Interactive effect of salinity and silver nanoparticles on photosynthetic and biochemical parameters of wheat. *Arch. Agron. Soil Sci.* **2017**, *63* (12), 1736−1747.
(44) Wei, C.; Zhang, Y.; Guo, J.; Han, B.; Yang, X.; Yuan, J. Effects of silica nanoparticles on growth and photosynthetic pigment contents of Scenedesmus obliquus. *J. Environ. Sci.* **2010**, *22* (1), 155−160.
(45) Ashkavand, P.; Tabari, M.; Zarafshar, M.; Tomášková, I.; Struve, D. Effect of SiO_2 nanoparticles on drought resistance in Hawthorn seedlings. *For. Res. Pap.* **2015**, *76* (4), 350−359.
(46) Xie, Y.; Li, B.; Zhang, Q.; Zhang, C. Effects of Nano-Silicon Dioxide on Photosynthetic Fluorescence Characteristics of Indocalamus barbatus McClure. *J. Nanjing For. Univ., Nat. Sci. Ed.* **2012**, *2*, 59−63.
(47) Anjum, N. A.; Gill, S. S.; Duarte, A. C.; Pereira, E.; Ahmad, I. Silver nanoparticles in soil−plant systems. *J. Nanopart. Res.* **2013**, *15* (9), No. 1896, DOI: 10.1007/s11051-013-1896-7.
(48) Rizwan, M.; Ali, S.; Qayyum, M. F.; Ok, Y. S.; Adrees, M.; Ibrahim, M.; Zia-ur-Rehman, M.; Farid, M.; Abbas, F. undefined. *J. Hazard. Mater.* **2017**, *322*, 2−16.
(49) Kirschbaum, M. U. Does enhanced photosynthesis enhance growth? Lessons learned from CO2 enrichment studies. *Plant Physiol.* **2011**, *155* (1), 117−124.
(50) Johnston, H. J.; Hutchison, G.; Christensen, F. M.; Peters, S.; Hankin, S.; Stone, V. A review of the in vivo and in vitro toxicity of silver and gold particulates: Particle attributes and biological mechanisms responsible for the observed toxicity. *Crit. Rev. Toxicol.* **2010**, *40* (4), 328−346.
(51) Mishra, S.; Singh, H. B. Biosynthesized silver nanoparticles as a nanoweapon against phytopathogens: Exploring their scope and potential in agriculture. *Appl. Microbiol. Biotechnol.* **2015**, *99* (3), 1097−1107.
(52) Austin, L. A.; Kang, B.; Yen, C.; El-Sayed, M. A. Nuclear targeted silver Nanospheres perturb the cancer cell cycle differently than those of Nanogold. *Bioconjugate Chem.* **2011**, *22* (11), 2324−2331.
(53) Hackenberg, S.; Scherzed, A.; Kessler, M.; Hummel, S.; Technau, A.; Froelich, K.; Ginzkey, C.; Koehler, C.; Hagen, R.; Kleinsasser, N. Silver nanoparticles: Evaluation of DNA damage, toxicity and functional impairment in human mesenchymal stem cells. *Toxicol. Lett.* **2011**, *201* (1), 27−33.
(54) Sanpui, P.; Chattopadhyay, A.; Ghosh, S. S. Induction of Apoptosis in cancer cells at low silver Nanoparticle concentrations using Chitosan Nanocarrier. *ACS Appl. Mater. Interfaces* **2011**, *3* (2), 218−228.

https://doi.org/10.1021/acsomega.4c00550
ACS Omega 2024, 9, 35332−35347

(55) Nallathamby, P. D.; Xu, X. N. Study of cytotoxic and therapeutic effects of stable and purified silver nanoparticles on tumor cells. *Nanoscale* **2010**, *2* (6), 942.
(56) Miura, N.; Shinohara, Y. Cytotoxic effect and apoptosis induction by silver nanoparticles in Hela cells. *Biochem. Biophys. Res. Commun.* **2009**, *390* (3), 733−737.
(57) Ernst, E.; Rungby, J.; Baatrup, E. Ultrastructural localization of silver in rat testis and organ distribution of radioactive silver in the rat. *J. Appl. Toxicol.* **1991**, *11* (5), 317−321.
(58) Tiwari, D. K.; Jin, T.; Behari, J. Dose-dependent in-vivo toxicity assessment of silver nanoparticle in Wistar rats. *Toxicol. Mech. Methods* **2011**, *21* (1), 13−24.
(59) Cheng, X.; Zhang, W.; Ji, Y.; Meng, J.; Guo, H.; Liu, J.; Wu, X.; Xu, H. Revealing silver cytotoxicity using AU nanorods/Ag shell nanostructures: Disrupting cell membrane and causing apoptosis through oxidative damage. *RSC Adv.* **2013**, *3* (7), 2296.
(60) Shen, X.; Zhou, Y.; Duan, L.; Li, Z.; Eneji, A. E.; Li, J. Silicon effects on photosynthesis and antioxidant parameters of soybean seedlings under drought and ultraviolet-B radiation. *J. Plant Physiol.* **2010**, *167* (15), 1248−1252.
(61) Hideg, E.; Takátsy, A.; Sár, C. P.; Vass, I.; Hideg, K. Utilizing new adamantyl spin traps in studying UV-B-induced oxidative damage of photosystem II. *J. Photochem. Photobiol., B* **1999**, *48* (2−3), 174−179.
(62) Desikan, R.; A-H-Mackerness, S.; Hancock, J. T.; Neill, S. J. Regulation of the arabidopsis Transcriptome by oxidative stress. *Plant Physiol.* **2001**, *127* (1), 159−172.
(63) Neill, S. Hydrogen peroxide signalling. *Curr. Opin. Plant Biol.* **2002**, *5* (5), 388−395.
(64) Yan, J.; Tsuichihara, N.; Etoh, T.; Iwai, S. Reactive oxygen species and nitric oxide are involved in ABA inhibition of stomatal opening. *Plant, Cell Environ.* **2007**, *30* (10), 1320−1325.
(65) Khan, M. N.; Mobin, M.; Abbas, Z. K.; AlMutairi, K. A.; Siddiqui, Z. H. Role of nanomaterials in plants under challenging environments. *Plant Physiol. Biochem.* **2017**, *110*, 194−209.
(66) Rico, C. M.; Hong, J.; Morales, M. I.; Zhao, L.; Barrios, A. C.; Zhang, J.; Peralta-Videa, J. R.; Gardea-Torresdey, J. L. Effect of cerium oxide nanoparticles on rice: A study involving the antioxidant defense system and in vivo fluorescence imaging. *Environ. Sci. Technol.* **2013**, *47* (11), 5635−5642.
(67) Wei, H.; Wang, E. Nanomaterials with enzyme-like characteristics (nanozymes): Next-generation artificial enzymes. *Chem. Soc. Rev.* **2013**, *42* (14), 6060.
(68) Lin, D.; Xing, B. Phytotoxicity of nanoparticles: Inhibition of seed germination and root growth. *Environ. Pollut.* **2007**, *150* (2), 243−250.
(69) Noctor, G.; Foyer, C. H. Ascorbate and GLUTATHIONE: Keeping active oxygen under control. *Annu. Rev. Plant Physiol. Plant Mol. Biol.* **1998**, *49* (1), 249−279.
(70) Mittler, R. ROS are good. *Trends Plant Sci.* **2017**, *22* (1), 11−19.
(71) Zaefyzadeh, M.; Quliyev, R. A.; Babayeva, S.; Abbasov, M. A. The effect of the interaction between genotypes and drought stress on the superoxide Dismutase and chlorophyll content in durum wheat landraces. *Turk. J. Biol.* **2009**, *33*, 1−7, DOI: 10.3906/biy-0801-12.
(72) Chen, Q.; Zhang, M.; Shen, S. Effect of salt on malondialdehyde and antioxidant enzymes in seedling roots of Jerusalem artichoke (*Helianthus tuberosus* L.). *Acta Physiol. Plant.* **2011**, *33* (2), 273−278.
(73) Bendary, E.; Francis, R.; Ali, H.; Sarwat, M.; El Hady, S. Antioxidant and structure−activity relationships (SARs) of some phenolic and anilines compounds. *Ann. Agric. Sci.* **2013**, *58* (2), 173−181.
(74) Côté, J.; Caillet, S.; Doyon, G.; Sylvain, J.; Lacroix, M. Bioactive compounds in cranberries and their biological properties. *Crit. Rev. Food Sci. Nutr.* **2010**, *50* (7), 666−679.
(75) Pratyusha, S. Phenolic compounds in the plant development and defense: An overview. *Plant Stress Physiol. - Perspect. Agric.* **2022**, 125−140, DOI: 10.5772/intechopen.102873.
(76) Joshi, P. K.; Saxena, S. C.; Arora, S. Characterization of brassica juncea antioxidant potential under salinity stress. *Acta Physiol. Plant.* **2011**, *33* (3), 811−822.
(77) Monreal, J.; Jiménez, E.; Remesal, E.; Morillo-Velarde, R.; García-Mauriño, S.; Echevarría, C. Proline content of sugar beet storage roots: Response to water deficit and nitrogen fertilization at field conditions. *Environ. Exp. Bot.* **2007**, *60* (2), 257−267.
(78) Zhu, M.; Ou, X.; Tang, J.; Shi, T.; Ma, X.; Wang, Y.; Wu, X.; Li, Q. X.; Hua, R. Uptake, distribution and translocation of imidacloprid-loaded fluorescence double hollow shell mesoporous silica nanoparticles and metabolism of imidacloprid in pakchoi. *Sci. Total Environ.* **2021**, *787*, No. 147578.
(79) Guidi, L.; Lo Piccolo, E.; Landi, M. Chlorophyll fluorescence, Photoinhibition and abiotic stress: Does it make any difference the fact to be a C3 or C4 species? *Front. Plant Sci.* **2019**, *10*, No. 174, DOI: 10.3389/fpls.2019.00174.
(80) Baker, N. R. Photoinhibition of photosynthesis. *Light Energy Source Information Carrier Plant Physiol.* **1996**, 89−97.
(81) Powles, S. B. Photoinhibition of photosynthesis induced by visible light. *Annu. Rev. Plant Physiol.* **1984**, *35* (1), 15−44.
(82) Aro, E.-M.; Virgin, I.; Andersson, B. Photoinhibition of Photosystem II. Inactivation, protein damage and turnover. *Biochim. Biophys. Acta, Bioenerg.* **1993**, *1143* (2), 113−134.
(83) Murata, N.; Takahashi, S.; Nishiyama, Y.; Allakhverdiev, S. I. Photoinhibition of photosystem II under environmental stress. *Biochim. Biophys. Acta, Bioenerg.* **2007**, *1767* (6), 414−421.

https://doi.org/10.1021/acsomega.4c00550
ACS Omega 2024, 9, 35332−35347